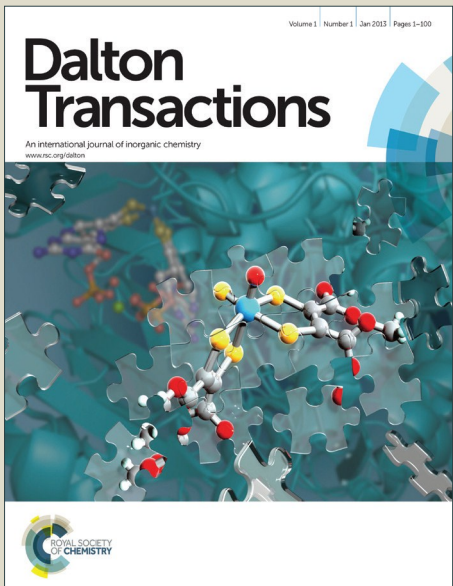


Dalton Transactions

Accepted Manuscript



This is an Accepted Manuscript, which has been through the Royal Society of Chemistry peer review process and has been accepted for publication.

Accepted Manuscripts are published online shortly after acceptance, before technical editing, formatting and proof reading. Using this free service, authors can make their results available to the community, in citable form, before we publish the edited article. We will replace this Accepted Manuscript with the edited and formatted Advance Article as soon as it is available.

You can find more information about Accepted Manuscripts in the [Information for Authors](#).

Please note that technical editing may introduce minor changes to the text and/or graphics, which may alter content. The journal's standard [Terms & Conditions](#) and the [Ethical guidelines](#) still apply. In no event shall the Royal Society of Chemistry be held responsible for any errors or omissions in this Accepted Manuscript or any consequences arising from the use of any information it contains.



p-Tolylimido rhenium(V) complexes with phenolate-based ligands: synthesis, X-ray studies and catalytic activity in oxidation with *tert*-butylhydroperoxide †

Izabela Gryca,^a Barbara Machura,^{*a} Jan Grzegorz Małecki,^a Joachim Kusz,^b Lidia S. Shul'pina,^c Nikolay S. Ikonnikov^c and Georgiy B. Shul'pin ^{*d,e}

Footnote:

^a Department of Crystallography, Institute of Chemistry, University of Silesia, 9th Szkołna St., 40-006 Katowice, Poland. E-mail: basia@ich.us.edu.pl

^b Institute of Physics, University of Silesia, 40-007 Katowice, Poland

^c Nesmeyanov Institute of Organoelement Compounds, Russian Academy of Sciences, ulitsa Vavilova, dom 28, Moscow 119991, Russia

^d Semenov Institute of Chemical Physics, Russian Academy of Sciences, ulitsa Kosygina, dom 4, Moscow 119991, Russia. E-mail: Shulpin@chph.ras.ru

^e Plekhanov Russian University of Economics, Stremyannyi pereulok, dom 36, Moscow 117997, Russia

† Electronic supplementary information (ESI, Figures and Tables) available: CCDC (numbers 1422176–1422188). For ESI and crystallographic data in CIF or other electronic format, see DOI: 10.1039/xxxxxxxxx

<Abstract> The reactions of *mer*-[Re(*p*-NTol)X₃(PPh₃)₂] (X = Cl, Br) with chelating phenolate-based ligands (2-(2-hydroxy-5-methylphenyl)benzotriazole (HL¹), 2-(2-hydroxyphenyl)benzothiazole (HL²) or 2-(2-hydroxyphenyl)benzoxazole (HL³)) afforded a series of *p*-tolylimido rhenium(V) complexes *cis*- or *trans* -(X,X)-[Re(*p*-NTol)X₂(L)(PPh₃)₂]_yMeCN (where X = Cl, Br; L = L¹, L², L³ and y = 0–2) and [Re(*p*-NTol)X(L)(PPh₃)₂]Z·*p*PPh₃ (where X = ReO₄, PF₆; L = L¹, L², L³ and *p* = 0 or 1). The reported compounds were characterized by elemental analysis FT-IR, NMR (¹H, ¹³C and ³¹P) and X-ray crystallography. Interestingly, halide ions of [Re(*p*-NTol)Cl₂(L¹)(PPh₃)₂]·MeCN (**1**) and [Re(*p*-NTol)Cl₂(L²)(PPh₃)₂]·2MeCN (**3**) are in *cis* relative

dispositions, whereas the complexes $[\text{Re}(p\text{-NTol})\text{Br}_2(\text{L})(\text{PPh}_3)]$ (L^1 for **2**, L^2 for **4** and L^3 for **6**) and $[\text{Re}(p\text{-NTol})\text{Cl}_2(\text{L}^3)(\text{PPh}_3)]$ (**5**) were found to be *trans*-(X,X) isomers. The compounds $[\text{Re}(p\text{-NTol})\text{X}(\text{L})(\text{PPh}_3)_2](\text{PF}_6)$ ($\text{X} = \text{Cl}, \text{Br}; \text{L} = \text{L}^1 \text{ and } \text{L}^2$) and $[\text{Re}(p\text{-NTol})\text{X}(\text{L}^3)(\text{PPh}_3)_2](\text{PF}_6)\text{PPh}_3$ ($\text{X} = \text{Cl}, \text{Br}$) have been tested in oxidative catalysis. A few compounds exhibited very good catalytic properties in oxidation of alcohols with *tert*-BuOOH (TBHP) in acetonitrile solution at moderate temperatures. Complex $[\text{Re}(p\text{-NTol})\text{Cl}(\text{L}^2)(\text{PPh}_3)_2]\text{PF}_6$ (**13**) is the catalyst of choice for oxidation of 1-phenylethanol to acetophenone (in 80% yield; turnover number attained 290 after 30 h) and cyclooctanol to cyclooctanone (in 88% yield). Notably lower activity has been found in the oxidation of alkanes with TBHP. Product distribution in the oxidation of methylcyclohexane indicates some sterical hindrance around the reaction center.

1. Introduction

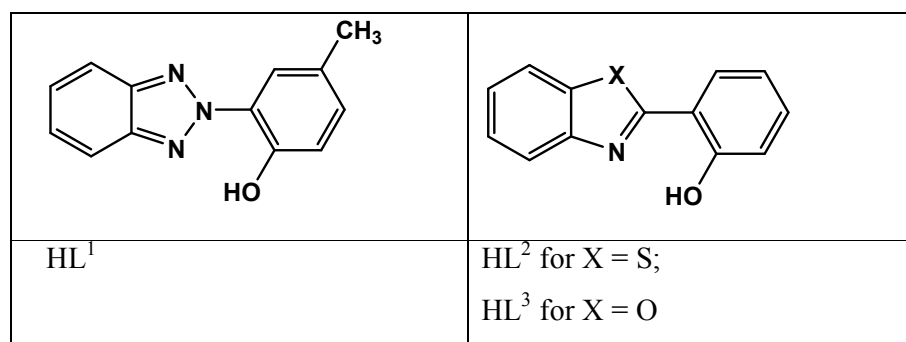
The chemistry of transition metal complexes containing multiple bonds to nitrogen atoms is currently the subject of intensive research. Such complexes have been successfully employed in the nitrogen fixation,¹ catalytic hydroamination of alkynes,² hydrosilylation of ketones and aldehydes,³ synthesis of various nitrogen heterocycles,⁴ activation of hydrocarbons including methane⁵ and in cycloaddition reactions with unsaturated organic substrates.⁶

Reported by Chatt and Rowe in 1962, first Re arylimido complexes $[\text{ReCl}_3(\text{NAr})(\text{PPh}_3)_2]$ were obtained in the reactions of $[\text{ReOCl}_3(\text{PPh}_3)_2]$ and aniline as the source of the imido ligand.⁷ Since then, many other valuable synthetic methodologies to imido rhenium complexes have been developed, including the reactions of oxo complexes with isocyanates ArNCO,⁸ phosphinimines RN=PPh (R=alkyl or aryl),⁹ arylazopyridines $\text{YC}_6\text{H}_4\text{-N}=\text{NC}_5\text{H}_4\text{N}$ (Y = H, 3-Me, 4-Me, 4-C1),¹⁰ silylamines RN(SiMe₃)₂,¹¹ hydrazines¹² as well as alkylation or arylation of nitrido complexes,¹³ thermolysis of alkyliminoalkyl metal complexes¹⁴ and the homolytic cleavage and addition of azo compounds.¹⁵ The synthesis of imido complexes directly from perrhenate is an essential step for any complexes to have viability as radiopharmaceuticals, as the emitting radionuclides ¹⁸⁶Re (1.07 MeV β-emitter, $t_{1/2} = 90\text{h}$) and ¹⁸⁸Re (2.12 MeV β-emitter, $t_{1/2} = 17\text{ h}$) are isolated as perrhenate ion from a ¹⁸⁸W generator system.¹⁶ Another convenient synthetic strategy for making imido complexes of rhenium concerns ligand exchange reactions with retention of the imido moiety.¹⁷

Our recent research has demonstrated that compounds $[\text{Re}(p\text{-NTol})\text{X}_3(\text{PPh}_3)_2]$ ($\text{X} = \text{Cl}, \text{Br}$) are versatile starting materials in the synthesis of Re imido complexes incorporating uninegative N,O-donor ligands.¹⁸ The studies revealed that the geometry of the resulted $[\text{Re}(p\text{-NTol})\text{X}_2(\text{L})(\text{PPh}_3)]$ ($\text{HL} = \text{pyridine-2-carboxylic acid, pyrazine-2-carboxylic acid, indazole-3-carboxylic acid and quinoline-2-carboxylic acid}$) complexes may be tuned by careful selection of chelating carboxylate-based ligands (steric and electronic properties) as well as experimental conditions. What is more, the results confirmed

that different regio-isomers might have a significant influence on catalyst activity. The complexes $[\text{Re}(p\text{-NTol})\text{X}_2(\text{pyz-2-COO})(\text{PPh}_3)]$ and $[\text{Re}(p\text{-NTol})\text{X}_2(\text{ind-3-COO})(\text{PPh}_3)]$ have been found to catalyze oxidation of alkanes with H_2O_2 and *tert*-butyl hydroperoxide (TBHP) and of alcohols with TBHP,^{18a} whereas the catalytic activity of $[\text{Re}(p\text{-NTol})\text{X}_2(\text{py-2-COO})(\text{PPh}_3)]$ was demonstrated in the synthesis of *N*-substituted ethyl glycine esters from ethyl diazoacetate and amines.^{18b}

To obtain other catalytically active imido rhenium compounds and get a deeper understanding of the isomeric preferences in the group of $[\text{Re}(p\text{-NTol})\text{X}_2(\text{L})(\text{PPh}_3)]$ we decided to carry out more in-depth investigations of imido rhenium complexes $[\text{Re}(p\text{-NTol})\text{X}_2(\text{L})(\text{PPh}_3)]$ incorporating phenolate-based chelating ligands: 2-(2-hydroxy-5-methylphenyl)benzotriazole (HL^1), 2-(2-hydroxyphenyl)benzothiazole (HL^2), 2-(2-hydroxyphenyl)benzoxazole (HL^3) (Scheme 1).



Scheme 1 Phenolate-based ligands employed in this study.

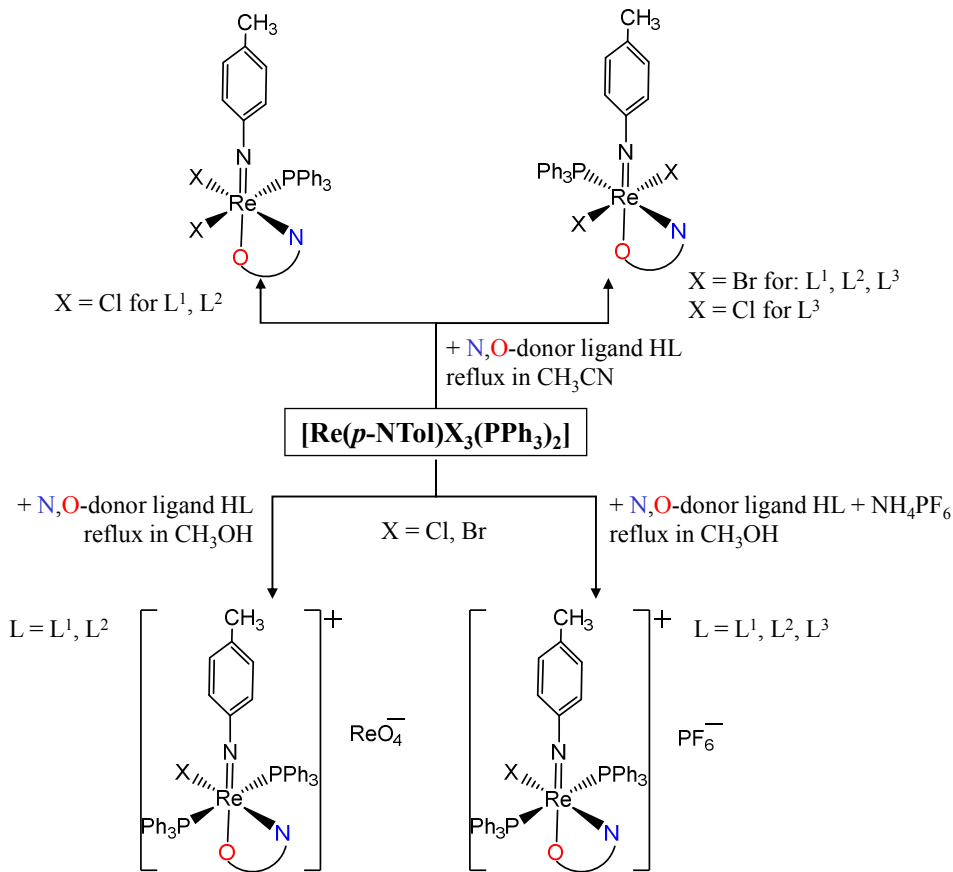
X-Ray structure of *cis*-(Cl,Cl)- $[\text{Re}(p\text{-NTol})\text{Cl}_2(\text{L}^1)(\text{PPh}_3)]\text{MeCN}$ (**1**) was reported in the previous paper.^{18d} The present contribution covers the synthesis, X-Ray structure and spectroscopy of the following new imido complexes: *trans*-(Br,Br)- $[\text{Re}(p\text{-NTol})\text{Br}_2(\text{L})(\text{PPh}_3)]$ (L^1 for **2**, L^2 for **4** and L^3 for **6**), *cis*-(Cl,Cl)- $[\text{Re}(p\text{-NTol})\text{Cl}_2(\text{L}^2)(\text{PPh}_3)]\text{2MeCN}$ (**3**) and *trans*-(Cl,Cl)- $[\text{Re}(p\text{-NTol})\text{Cl}_2(\text{L}^3)(\text{PPh}_3)]$ (**5**), $[\text{Re}(p\text{-NTol})\text{Cl}(\text{L})(\text{PPh}_3)_2]\text{ReO}_4$ (L^1 for **7** and L^2 for **9**), $[\text{Re}(p\text{-NTol})\text{Br}(\text{L}^1)(\text{PPh}_3)_2]\text{ReO}_4$ (**8**), $[\text{Re}(p\text{-NTol})\text{Br}(\text{L}^2)(\text{PPh}_3)_2]\text{ReO}_4\text{:PPh}_3$ (**10**), $[\text{Re}(p\text{-NTol})\text{Cl}(\text{L})(\text{PPh}_3)_2]\text{PF}_6$ (L^1 for **11** and L^2 for **13**), $[\text{Re}(p\text{-NTol})\text{Br}(\text{L})(\text{PPh}_3)_2]\text{PF}_6$ (L^1 for **12** and L^2 for **14**) and $[\text{Re}(p\text{-NTol})\text{X}(\text{L}^3)(\text{PPh}_3)_2]\text{PF}_6\text{:PPh}_3$ (Cl for **15** and Br for **16**).

2. Results and discussion

2.1 Synthesis of the complexes

The complexes *cis*- or *trans*-(X,X)- $[\text{Re}(p\text{-NTol})\text{X}_2(\text{L})(\text{PPh}_3)]\bullet y\text{MeCN}$ (where X = Cl, Br; L = L^1 , L^2 , L^3 and $y = 0\text{--}2$) and $[\text{Re}(p\text{-NTol})\text{X}(\text{L})(\text{PPh}_3)_2]\text{Z}\bullet p\text{PPh}_3$ (where X = Cl, Br; Z = ReO_4 , PF_6 ; L = L^1 , L^2 , L^3 and $p = 0$ or 1) were prepared by reacting of *mer*- $[\text{Re}(p\text{-NTol})\text{X}_3(\text{PPh}_3)_2]$ (X = Cl, Br) and 2-(2-hydroxy-

5-methylphenyl)benzotriazole (HL^1), 2-(2-hydroxyphenyl)benzothiazole (HL^2) or 2-(2-hydroxyphenyl)benzoxazole (HL^3). The synthetic strategy of **1–16** is presented in Scheme 2.



Scheme 2 Formation of complexes **1–16**.

As shown in Scheme 2, the solvent seems to play a crucial role in the determination of activation energetics and reaction kinetics and thermodynamics, and thus the resultant structures of imido Re complexes incorporating L^1 , L^2 and L^3 ligands.

The reactions between *mer*- $[\text{Re}(p\text{-NTol})\text{X}_3(\text{PPh}_3)_2]$ and 2-(2-hydroxy-5-methylphenyl)benzotriazole (HL^1), 2-(2-hydroxyphenyl)benzothiazole (HL^2) or 2-(2-hydroxyphenyl)benzoxazole (HL^3) in acetonitrile resulted in the formation of monosubstituted compounds of formula $[\text{Re}(p\text{-NTol})\text{X}_2(\text{L})(\text{PPh}_3)]$.

Interestingly, the halide ions of $[\text{Re}(p\text{-NTol})\text{Cl}_2(\text{L}^1)(\text{PPh}_3)]\cdot\text{MeCN}$ (**1**) and $[\text{Re}(p\text{-NTol})\text{Cl}_2(\text{L}^2)(\text{PPh}_3)]\cdot 2\text{MeCN}$ (**3**) are arranged in *cis* geometry, whereas X^- ligands of $[\text{Re}(p\text{-NTol})\text{Br}_2(\text{L})(\text{PPh}_3)]$ (L^1 for **2**, L^2 for **4** and L^3 for **6**) and $[\text{Re}(p\text{-NTol})\text{Cl}_2(\text{L}^3)(\text{PPh}_3)]$ (**5**) occupy *trans* positions to each other. The *trans-cis* rearrangement must take place during the chelation step, no *cis-trans* isomerism in solution was evidenced by NMR studies for the reported $[\text{Re}(p\text{-NTol})\text{X}_2(\text{L})(\text{PPh}_3)]$. It is likely that electronic effects resulting from differences in ionic radii, polarizabilities and donor

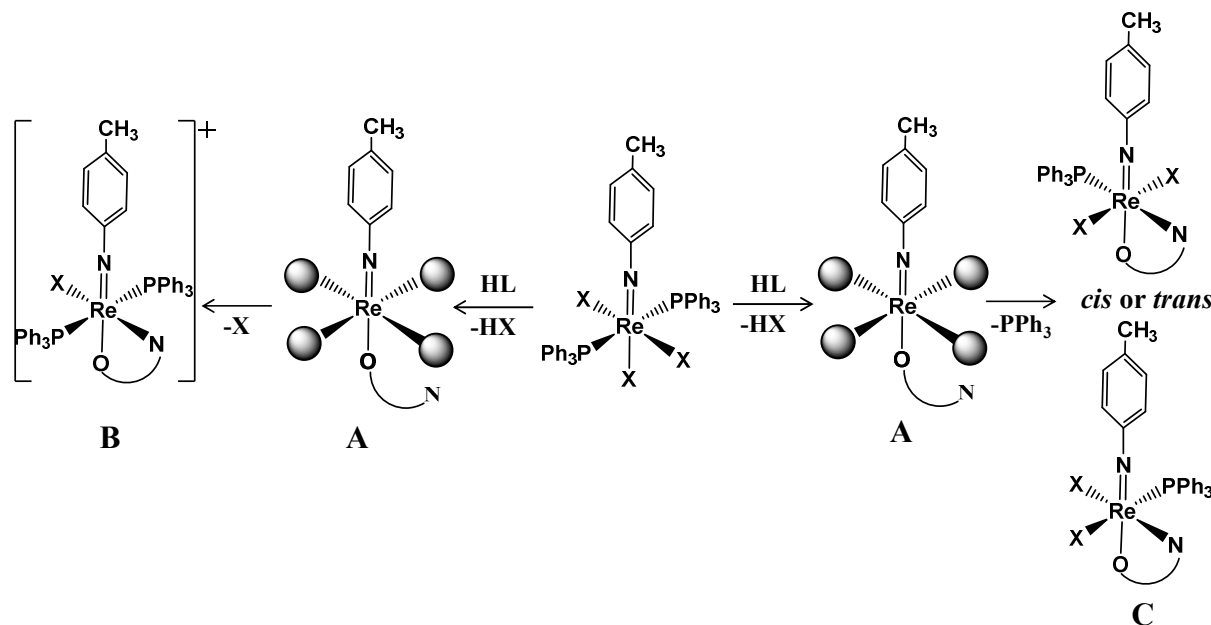
availability of bromide compared to chloride ligands are significant factors responsible for isomeric preferences in the group of complexes $[\text{Re}(p\text{-Ntol})\text{X}_2(\text{L})(\text{PPh}_3)]$ incorporating L^1 and L^2 ligands (*cis*-(Cl,Cl)- $[\text{Re}(p\text{-NTol})\text{Cl}_2(\text{L})(\text{PPh}_3)]$ and *trans*-(Br,Br)- $[\text{Re}(p\text{-NTol})\text{Br}_2(\text{L})(\text{PPh}_3)]$). In turn, isomeric form (*trans-cis*) of $[\text{Re}(p\text{-NTol})\text{X}_2(\text{L}^3)(\text{PPh}_3)]$ seems to be mainly controlled by electronic factors of the chelating ligand. In this case, both chloride and bromide analogues form *trans*-(X,X)-isomers. The findings concerning $[\text{Re}(p\text{-NTol})\text{X}_2(\text{L}^3)(\text{PPh}_3)]$ are consistent with those reported for *trans*-(X,X)- $[\text{Re}(p\text{-NTol})\text{X}_2(\text{pyz-2-COO})(\text{PPh}_3)]$ and *cis*-(X,X)- $[\text{Re}(p\text{-NTol})\text{X}_2(\text{ind-3-COO})(\text{PPh}_3)]$,^{18a} for which the final structure was independent on halide ions but influenced by the chelating ligand. On contrary, formation of *trans/cis*-(X,X) isomers of $[\text{Re}(p\text{-NTol})\text{X}_2(\text{py-2-COO})(\text{PPh}_3)]$ was found to be solvent-dependent. Refluxing of $[\text{Re}(p\text{-NTol})\text{X}_3(\text{PPh}_3)_2]$ with py-2-COOH in methanol led to a mixture of the compounds *trans*-(X,X)- $[\text{Re}(p\text{-NTol})\text{X}_2(\text{py-2-COO})(\text{PPh}_3)]$ and *cis*-(X,X)- $[\text{Re}(p\text{-NTol})\text{X}_2(\text{py-2-COO})(\text{PPh}_3)]$, whereas the same reactions in methanol resulted in the formation of *trans*-(X,X)- $[\text{Re}(p\text{-NTol})\text{X}_2(\text{py-2-COO})(\text{PPh}_3)]$.^{18b}

Compared with the rhenium(V) imido complexes of carboxylate-based ligands,^{18a-c} the reactivity of $[\text{Re}(p\text{-NTol})\text{X}_3(\text{PPh}_3)_2]$ with phenolate-based ligands in methanol was considerably different. In this case, two kinds of products $[\text{Re}(p\text{-NTol})\text{X}(\text{L})(\text{PPh}_3)_2]\text{ReO}_4$ and $[\text{Re}(p\text{-NTol})\text{X}(\text{L})(\text{PPh}_3)_2]\text{PF}_6$ were isolated depending on experimental conditions. Addition of NH_4PF_6 salt led to formation of $[\text{Re}(p\text{-NTol})\text{X}(\text{L})(\text{PPh}_3)_2]\text{PF}_6$, whereas refluxing of $[\text{Re}(p\text{-NTol})\text{X}_3(\text{PPh}_3)_2]$ with phenolate-based ligands (HL^1 , HL^2 and HL^3) in methanol followed by slow solvent evaporation at room temperature resulted in isolation of $[\text{Re}(p\text{-NTol})\text{X}(\text{L})(\text{PPh}_3)_2]\text{ReO}_4$. The origin of the perrhenate anion in $[\text{Re}(p\text{-NTol})\text{X}(\text{L})(\text{PPh}_3)_2]\text{ReO}_4$ is probably due to the oxidation of a portion of $[\text{Re}(p\text{-NTol})\text{X}(\text{L})(\text{PPh}_3)_2]\text{X}$ ($\text{X} = \text{Cl}, \text{Br}$), which is supposed to form in the first step of the reaction. The formation of perrhenate is well documented in the chemistry of rhenium(V) complexes and was confirmed previously for $[\text{Re}(p\text{-NTol})(\text{hmbzim})_2(\text{PPh}_3)]\text{ReO}_4$,¹⁹ $[\text{ReOCl}_2(\text{pzH})_2(\text{OAsPh}_3)](\text{ReO}_4)$,²⁰ $[\text{ReO}(\text{hmbzim})_2(\text{PPh}_3)](\text{ReO}_4)$,²¹ $[\text{Re}(p\text{-NTol})\text{X}(\text{OMe})(\text{Hdpa})(\text{PPh}_3)]\text{ReO}_4$.²²

In both acetonitrile and methanol, the initial step of the complex formation seems to concern the substitution of the oxygen atom of N,O-donor ligand (HL^1 , HL^2 and HL^3) for the labile X ligand *trans* to imido group in $[\text{Re}(p\text{-NTol})\text{X}_3(\text{PPh}_3)_2]$, possibly with the proton transfer to give monodentate intermediate A (Scheme 3). In the next step, the uncoordinated N-donor atom of N,O-donor ligand would either substitute the equatorial halide to form a monocationic complexes $[\text{Re}(p\text{-NTol})\text{X}(\text{L})(\text{PPh}_3)_2]\text{X}$ or substitute one of the equatorial phosphine ligands to form neutral imido complexes *trans*-(X,X)- $[\text{Re}(p\text{-NTol})\text{X}_2(\text{L})(\text{PPh}_3)]$ or *cis*-(X,X)- $[\text{Re}(p\text{-NTol})\text{X}_2(\text{N-O})(\text{PPh}_3)]$. For reported here uninegative N,O-donor ligands (L^1 , L^2 and L^3), both neutral $[\text{Re}(p\text{-NTol})\text{X}_2(\text{L})(\text{PPh}_3)]$ and cationic $[\text{Re}(p\text{-NTol})\text{X}(\text{L})(\text{PPh}_3)_2]^+$

complexes were obtained. On the contrary, the reactions of $[\text{Re}(p\text{-NTol})\text{X}_3(\text{PPh}_3)_2]$ with chelating carboxylate-based ligands^{18a–c} resulted in formation of only neutral $[\text{Re}(p\text{-NTol})\text{X}_2(\text{L})(\text{PPh}_3)]$.

Taken together, the studies support that final molecular structure of imido rhenium(V) complexes incorporating uninegative N,O-donor ligands may be tuned by careful selection of L and X ligands as well as experimental conditions. To get a deeper understanding this relationship, however, more research needs to be undertaken.



Scheme 3. Proposed mechanism for the formation of *cis* or *trans*-(X,X)- $[\text{Re}(p\text{-NTol})\text{X}_2(\text{L})(\text{PPh}_3)]$ and $[\text{Re}(p\text{-NTol})\text{X}(\text{L})(\text{PPh}_3)_2]^+$.

2.2 Molecular Structures

The crystallographic data of compounds **2–10** and **13–16** are summarized in Tables 1–3, and the selected bond lengths and angles are gathered in Tables 4–6. The representative molecular structures of $[\text{Re}(p\text{-NTol})\text{X}_2(\text{L})(\text{PPh}_3)]$, $[\text{Re}(p\text{-NTol})\text{X}(\text{L})(\text{PPh}_3)_2]\text{ReO}_4$ and $[\text{Re}(p\text{-NTol})\text{X}(\text{L})(\text{PPh}_3)_2]\text{PF}_6$ are shown in Fig. 1. The preservative views of molecular structures for remaining compounds were included in the Electronic supplementary information (ESI; Figs. S1–S3).

Table 1 Crystal data and structure refinement for complexes **2–6**

	2	3	4	5	6
Empirical formula	C ₃₈ H ₃₂ Br ₂ N ₄ OPRe	C ₄₂ H ₃₆ Cl ₂ N ₄ OSPRe	C ₃₈ H ₃₀ Br ₂ N ₂ OPSRe	C ₃₈ H ₃₀ Cl ₂ N ₂ O ₂ PRE	C ₃₈ H ₃₀ Br ₂ N ₂ O ₂ PRE
Formula weight	937.67	932.88	939.69	834.71	923.63
Temperature [K]	293.0(2)	293.0(2)	293.0(2)	298.0(1)	293.0(2)
Wavelength [Å]	0.71073	0.71073	0.71073	0.71073	0.71073
Crystal system	monoclinic	triclinic	monoclinic	monoclinic	monoclinic
Space group	P2 ₁ /n	P-1	P2 ₁ /n	P2 ₁ /n	P2 ₁ /c
Unit cell dimensions [Å, °]	a = 10.1990(4) b = 22.6461(8) c = 14.8400(6) β = 90.964(3)	a = 10.4203(4) b = 11.1922(4) c = 17.5181(6) α = 80.298(3) β = 86.888(3) γ = 74.343(3)	a = 10.0403(4) b = 22.9911(8) c = 14.5963(5) β = 91.736(3)	a = 9.9154(10) b = 22.4996(3) c = 14.6664(2) β = 92.8070(10)	a = 10.0301(3) b = 22.6557(7) c = 17.5430(4) β = 122.839(2)
Volume [Å ³]	3427.1(2)	1939.04(12)	3367.8(2)	3268.04(7)	3349.42(16)
Z	4	2	4	4	4
Density (calculated) [Mg/m ³]	1.817	1.598	1.853	1.697	1.832
Absorption coefficient [mm ⁻¹]	5.962	3.405	6.125	3.969	6.099
F(000)	1824	928	1824	1648	1792
Crystal size [mm]	0.064 x 0.069 x 0.094	0.035 x 0.079 x 0.083	0.037 x 0.049 x 0.118	0.060 x 0.120 x 0.380	0.104 x 0.089 x 0.057
θ range for data collection [°]	3.36 to 25.00	3.54 to 25.00	3.31 to 25.00	2.59 to 25.68	3.38 to 25.00
Index ranges	-12 ≤ h ≤ 10 -26 ≤ k ≤ 26 -17 ≤ l ≤ 15	-11 ≤ h ≤ 12 -13 ≤ k ≤ 13 -20 ≤ l ≤ 20	-11 ≤ h ≤ 11 -27 ≤ k ≤ 26 -16 ≤ l ≤ 17	-12 ≤ h ≤ 9 -27 ≤ k ≤ 27 -17 ≤ l ≤ 17	-11 ≤ h ≤ 11 -26 ≤ k ≤ 23 -17 ≤ l ≤ 16
Reflections collected	19225	14656	17314	14764	17713
Independent reflections	6030 (R _{int} = 0.0450)	6821 (R _{int} = 0.0621)	5914 (R _{int} = 0.0372)	6152 (R _{int} = 0.0298)	5877 (R _{int} = 0.0377)
Completeness to 2θ=50° [%]	99.8	99.7	99.7	99.7	99.7
Max. and min. transmission	0.277 and 1.000	0.789 and 1.000	0.466 and 1.000	0.690 and 1.000	0.403 and 1.000
Data / restraints / parameters	6030 / 0 / 426	6821 / 0 / 472	5914 / 0 / 416	6152 / 0 / 416	5877 / 0 / 416
Goodness-of-fit on F ²	1.065	0.954	1.029	0.920	1.029
Final R indices [I>2σ(I)]	R1 = 0.0321 wR2 = 0.0726	R1 = 0.0438 wR2 = 0.0837	R1 = 0.0270 wR2 = 0.0490	R1 = 0.0199	R1 = 0.0290 wR2 = 0.0640
R indices (all data)	R1 = 0.0433 wR2 = 0.0764	R1 = 0.0645 wR2 = 0.0884	R1 = 0.0398 wR2 = 0.0518	R1 = 0.0274	R1 = 0.0424 wR2 = 0.0673
Largest diff. peak and hole[e Å ⁻³]	1.236 and -0.773	1.799 and -0.996	0.709 and -0.440	0.875 and -0.749	0.776 and -0.995

Table 2 Crystal data and structure refinement for complexes **7–10**

	7	8	9	10
Empirical formula	C ₅₆ H ₄₇ ClN ₄ O ₅ P ₂ Re ₂	C ₅₆ H ₄₇ BrN ₄ O ₅ P ₂ Re ₂	C ₅₆ H ₄₅ ClN ₂ O ₅ P ₂ SRe ₂	C ₇₄ H ₆₀ BrN ₂ O ₅ P ₃ SRe ₂
Formula weight	1325.77	1370.23	1327.79	1634.52
Temperature [K]	293.0(2)	293.0(2)	293.0(2)	293.0(2)
Wavelength [Å]	0.71073	0.71073	0.71073	0.71073
Crystal system	monoclinic	monoclinic	monoclinic	triclinic
Space group	P2 ₁ /n	P2 ₁ /n	P2 ₁ /n	P-1
Unit cell dimensions [Å, °]	a = 12.7856(4) b = 20.8513(6) c = 20.5169(6) β = 108.012(3)	a = 12.8922(5) b = 20.9641(6) c = 20.6190(7) β = 106.991(4)	a = 12.7001(3) b = 21.0563(4) c = 19.9772(5) β = 107.282(3)	a = 11.6599(3) b = 17.4480(4) c = 18.3654(5) α = 99.887(2) β = 107.017(2) γ = 108.687(2) 3235.74(14)
Volume [Å ³]	5201.7(3)	5329.5(3)	5101.1(2)	3235.74(14)
Z	4	4	4	2
Density (calculated) [Mg/m ³]	1.693	1.730	1.729	1.678
Absorption coefficient [mm ⁻¹]	4.815	5.399	4.948	4.515
F(000)	2592	2664	2592	1608
Crystal size [mm]	0.040 x 0.082 x 0.181	0.092 x 0.138 x 0.168	0.028 x 0.082 x 0.177	0.114 x 0.116 x 0.161
θ range for data collection [°]	3.50 to 25.00	3.35 to 25.00	3.29 to 25.00	3.44 to 25.00
Index ranges	-15 ≤ h ≤ 15 -19 ≤ k ≤ 24 -24 ≤ l ≤ 19	-14 ≤ h ≤ 15 -24 ≤ k ≤ 24 -24 ≤ l ≤ 22	-15 ≤ h ≤ 15 -24 ≤ k ≤ 25 -23 ≤ l ≤ 23	-12 ≤ h ≤ 13 -20 ≤ k ≤ 20 -21 ≤ l ≤ 21
Reflections collected	28622	26577	27174	28741
Independent reflections	9141 (R _{int} = 0.033)	9371 (R _{int} = 0.0347)	8960 (R _{int} = 0.0323)	11365 (R _{int} = 0.0439)
Completeness to 2θ=50° [%]	99.7	99.7	99.8	99.8
Max. and min. transmission	0.497 and 1.000	0.644 and 1.000	0.454 and 1.000	0.370 and 1.000
Data / restraints / parameters	9141 / 0 / 633	9371 / 0 / 633	8960 / 0 / 623	11365 / 0 / 794
Goodness-of-fit on F ²	1.028	1.042	1.032	1.011
Final R indices [I>2σ(I)]	R1 = 0.0350 wR2 = 0.0756	R1 = 0.0439 wR2 = 0.0992	R1 = 0.0375 wR2 = 0.0843	R1 = 0.0337 wR2 = 0.0699
R indices (all data)	R1 = 0.0456 wR2 = 0.0794	R1 = 0.0620 wR2 = 0.1052	R1 = 0.0507 wR2 = 0.0887	R1 = 0.0467 wR2 = 0.0749
Largest diff. peak and hole[e Å ⁻³]	2.22 and -2.18	2.608 and -2.749	1.659 and -1.544	1.823 and -1.624

Table 3 Crystal data and structure refinement for complexes **13–16**

	13	14	15	16
Empirical formula	C ₅₆ H ₄₅ ClF ₆ N ₂ OP ₃ ReS	C ₅₆ H ₄₅ BrF ₆ N ₂ OP ₃ ReS	C ₇₄ H ₆₀ ClF ₆ N ₂ O ₂ P ₄ Re	C ₇₄ H ₆₀ BrF ₆ N ₂ O ₂ P ₄ Re
Formula weight	1222.56	1267.02	1468.77	1513.23
Temperature [K]	293.0(2)	293.0(2)	293.0(2)	293.0(2)
Wavelength [Å]	0.71073	0.71073	0.71073	0.71073
Crystal system	monoclinic	monoclinic	triclinic	triclinic
Space group	P2 ₁ /c	P2 ₁ /c	P-1	P-1
Unit cell dimensions [Å, °]	a = 12.2050(4) b = 11.5341(5) c = 36.2386(12) β = 91.344(3)	a = 12.1934(5) b = 11.6623(3) c = 36.0446(12) β = 91.283(4)	a = 11.7939(7) b = 17.2730(7) c = 18.3327(11) α = 99.156(4) β = 107.652(5) γ = 108.436(4)	a = 11.8734(3) b = 17.2825(5) c = 18.3204(5) α = 99.237(2) β = 107.373(2) γ = 108.801(2)
Volume [Å ³]	5100.1(3)	5124.4(3)	3239.1(3)	3256.39(15)
Z	4	4	2	2
Density (calculated) [Mg/m ³]	1.592	1.642	1.506	1.543
Absorption coefficient [mm ⁻¹]	2.635	3.350	2.082	2.644
F(000)	2440	2512	1480	1516
Crystal size [mm]	0.159 x 0.064 x 0.038	0.388 x 0.078 x 0.052	0.068 x 0.085 x 0.122	0.099 x 0.112 x 0.209
θ range for data collection [°]	3.28 to 25.00	3.49 to 25.00	3.36 to 25.00	3.35 to 25.00
Index ranges	-14<=h<=14 -13<=k<=13 -43<=l<=43	-14 ≤ h ≤ 14 -13 ≤ k ≤ 12 -42 ≤ l ≤ 36	-14 ≤ h ≤ 14 -20 ≤ k ≤ 20 -21 ≤ l ≤ 21	-13 ≤ h ≤ 14 -19 ≤ k ≤ 20 -21 ≤ l ≤ 21
Reflections collected	33240	33339	31414	30772
Independent reflections	8965 (R _{int} = 0.0963)	8996 (R _{int} = 0.0558)	11368 (R _{int} = 0.0889)	11445 (R _{int} = 0.0647)
Completeness to 2θ=50° [%]	99.8	99.7	99.8	99.8
Max. and min. transmission	0.420 and 1.000	0.562 and 1.000	0.817 and 1.000	0.619 and 1.000
Data / restraints / parameters	8965 / 0 / 641	8996 / 0 / 641	11368 / 0 / 812	11445 / 0 / 812
Goodness-of-fit on F ²	1.072	1.168	0.961	1.062
Final R indices [I>2σ(I)]	R1 = 0.0789 wR2 = 0.1525	R1 = 0.0525 wR2 = 0.0850	R1 = 0.0626 wR2 = 0.1306	R1 = 0.0473 wR2 = 0.0991
R indices (all data)	R1 = 0.1062 wR2 = 0.1617	R1 = 0.0657 wR2 = 0.0882	R1 = 0.1013 wR2 = 0.1443	R1 = 0.0661 wR2 = 0.1076
Largest diff. peak and hole[e Å ⁻³]	3.571 and -2.327	1.193 and -2.387	2.336 and -0.981	1.796 and -0.798

Table 4 The selected bond lengths [\AA] and angles [$^\circ$] for compounds **2–6**

	2 (X=Br)	3 (X=Cl)	4 (X=Br)	5 (X=Cl)	6 (X=Br)
Bond lengths					
Re(1)–N(2)	1.723(4)	1.704(5)	1.725(3)	1.721(2)	1.722(4)
Re(1)–O(1)	1.997(3)	2.008(4)	2.016(3)	2.0113(18)	2.004(3)
Re(1)–N(1)	2.181(4)	2.136(5)	2.186(3)	2.161(2)	2.160(4)
Re(1)–X(1)	2.5445(5)	2.4357(14)	2.5430(4)	2.4190(7)	2.5321(5)
Re(1)–X(2)	2.5610(5)	2.4142(16)	2.5732(4)	2.4014(7)	2.5545(5)
Re(1)–P(1)	2.4279(12)	2.4555(15)	2.4431(10)	2.4339(7)	2.4393(12)
Bond angles					
N(2)–Re(1)–O(1)	177.41(15)	173.54(19)	177.64(12)	177.32(9)	176.88(14)
N(2)–Re(1)–N(1)	96.04(16)	97.2(2)	96.65(13)	96.33(9)	96.12(15)
O(1)–Re(1)–N(1)	81.73(13)	81.78(18)	81.78(11)	81.56(8)	81.47(14)
N(2)–Re(1)–X(1)	94.46(13)	98.94(15)	93.36(10)	96.15(7)	93.63(11)
O(1)–Re(1)–X(1)	84.03(10)	87.35(11)	84.75(7)	85.46(6)	84.20(9)
N(1)–Re(1)–X(1)	84.73(10)	85.14(12)	84.36(8)	88.43(6)	84.43(10)
N(2)–Re(1)–X(2)	96.75(13)	93.15(17)	97.18(10)	94.13(7)	96.46(11)
O(1)–Re(1)–X(2)	84.52(10)	88.62(13)	84.55(7)	84.04(6)	85.45(9)
N(1)–Re(1)–X(2)	87.93(11)	167.71(13)	88.19(8)	84.30(6)	87.82(10)
X(1)–Re(1)–X(2)	167.181(19)	86.77(5)	167.733(15)	168.00(2)	167.878(18)
N(2)–Re(1)–P(1)	92.54(13)	88.83(15)	91.41(10)	91.66(8)	91.83(12)
O(1)–Re(1)–P(1)	89.64(10)	84.97(11)	90.05(8)	90.38(6)	90.49(9)
N(1)–Re(1)–P(1)	171.23(10)	97.00(12)	171.21(9)	171.61(6)	171.53(11)
X(1)–Re(1)–P(1)	92.82(3)	171.64(5)	91.69(3)	93.27(2)	92.17(3)
X(2)–Re(1)–P(1)	92.87(3)	89.75(5)	94.30(3)	92.60(2)	94.22(3)
C(32)–N(2)–Re(1)	174.3(3)	170.5(4)	173.8(3)	172.0(2)	172.4(3)

Table 5 The experimental bond lengths [Å] and angles [°] for compounds **7–10**

	7 (X=Cl)	8 (X=Br)	9 (X=Cl)	10 (X=Br)
Bond lengths				
Re(1)–N(2)	1.731(4)	1.741(5)	1.722(4)	1.732(3)
Re(1)–O(1)	1.972(3)	1.979(4)	1.983(3)	1.974(3)
Re(1)–N(1)	2.136(4)	2.149(5)	2.159(4)	2.147(4)
Re(1)–X(1)	2.3971(14)	2.5516(7)	2.4673(11)	2.5671(5)
Re(1)–P(1)	2.4984(13)	2.5127(17)	2.4956(13)	2.5179(10)
Re(1)–P(2)	2.5075(14)	2.5101(17)	2.5104(13)	2.5268(10)
Re(2)–O(2)	1.668(8)	1.600(11)	1.704(7)	1.696(4)
Re(2)–O(3)	1.653(9)	1.633(11)	1.690(7)	1.690(5)
Re(2)–O(4)	1.696(8)	1.681(7)	1.693(6)	1.642(5)
Re(2)–O(5)	1.683(6)	1.706(10)	1.659(8)	1.699(5)
Bond angles				
N(2)–Re(1)–O(1)	178.48(16)	177.6(2)	176.98(17)	175.76(14)
N(2)–Re(1)–N(1)	98.79(16)	99.5(2)	100.16(17)	100.59(15)
O(1)–Re(1)–N(1)	81.52(14)	81.64(18)	82.79(15)	83.30(13)
N(2)–Re(1)–X(1)	91.05(13)	90.32(16)	89.19(13)	88.78(12)
O(1)–Re(1)–X(1)	88.73(10)	88.72(12)	87.89(11)	87.36(9)
N(1)–Re(1)–X(1)	169.64(11)	169.50(14)	170.46(12)	170.60(9)
N(2)–Re(1)–P(1)	96.25(14)	92.15(17)	96.35(13)	95.25(10)
O(1)–Re(1)–P(1)	85.24(9)	85.68(13)	84.28(10)	86.38(8)
N(1)–Re(1)–P(1)	88.75(11)	91.70(14)	89.96(11)	90.18(8)
X(1)–Re(1)–P(1)	86.96(4)	91.71(4)	87.09(4)	88.19(3)
C(32)–N(2)–Re(1)	171.5(3)	171.6(5)	171.3(4)	168.5(3)
O(1)–Re(1)–P(2)	85.46(9)	85.37(13)	86.90(10)	87.48(8)
N(2)–Re(1)–P(2)	93.04(14)	96.77 (17)	92.33(13)	90.73(10)
N(1)–Re(1)–P(2)	91.96(11)	88.39(14)	91.46(11)	91.32(8)
P(1)–Re(1)–P(2)	170.46(4)	170.94(5)	170.82(4)	173.47(4)
P(2)–Re(1)–X(1)	90.74(4)	86.68(4)	90.05(4)	89.31(3)
O(2)–Re(2)–O(3)	110.9(5)	110.3(7)	109.5(4)	110.1(2)
O(2)–Re(2)–O(4)	108.8(4)	111.6(6)	109.8(3)	111.5(3)
O(2)–Re(2)–O(5)	109.9(4)	107.4(5)	108.7(4)	108.7(3)
O(3)–Re(2)–O(4)	109.9(5)	108.4(6)	107.6(3)	109.4(3)
O(3)–Re(2)–O(5)	108.2(4)	110.5(6)	108.9(5)	107.6(3)
O(4)–Re(2)–O(5)	109.1(4)	108.7(5)	112.3(4)	109.5(4)

Table 6 The selected experimental bond lengths [\AA] and angles [$^\circ$] for **13–16**

	13 (X=Cl)	14 (X=Br)	15 (X=Cl)	16 (X=Br)
Bond lengths				
Re(1)–N(2)	1.734(8)	1.717(5)	1.740(7)	1.731(5)
Re(1)–O(1)	2.002(7)	1.984(4)	1.979(5)	1.974(3)
Re(1)–N(1)	2.161(8)	2.163(5)	2.146(8)	2.141(5)
Re(1)–X(1)	2.409(3)	2.5607(7)	2.407(3)	2.5552(7)
Re(1)–P(1)	2.514(3)	2.5155(17)	2.517(2)	2.5201(16)
Re(1)–P(2)	2.512(3)	2.5160(16)	2.509(2)	2.5097(16)
P(3)–F(1)	1.512(13)	1.540(7)	1.576(11)	1.558(10)
P(3)–F(2)	1.551(11)	1.523(7)	1.501(13)	1.557(8)
P(3)–F(3)	1.525(11)	1.508(7)	1.531(11)	1.559(9)
P(3)–F(4)	1.538(10)	1.562(7)	1.566(11)	1.567(8)
P(3)–F(5)	1.560(11)	1.548(6)	1.533(13)	1.545(10)
P(3)–F(6)	1.531(13)	1.522(6)	1.587(14)	1.557(6)
P(3)–F(1A)			1.561(12)	1.557(9)
P(3)–F(2A)			1.586(10)	1.549(15)
P(3)–F(3A)			1.555(9)	1.553(9)
P(3)–F(4A)			1.553(12)	1.551(11)
P(3)–F(5A)			1.530(10)	1.563(10)
P(3)–F(6A)			1.579(10)	1.569(14)
Bond angles				
N(2)–Re(1)–O(1)	174.9(3)	174.1(2)	177.3(3)	176.97(19)
N(2)–Re(1)–N(1)	101.9(4)	102.9(2)	97.5(3)	98.3(2)
O(1)–Re(1)–N(1)	82.8(3)	82.58(18)	82.6(3)	82.50(17)
N(2)–Re(1)–X(1)	92.1(3)	91.35(16)	91.0(3)	90.40(18)
O(1)–Re(1)–X(1)	83.3(2)	83.25(12)	89.02(19)	88.93(11)
N(1)–Re(1)–X(1)	165.9(3)	165.57(14)	171.5(2)	171.29(14)
N(2)–Re(1)–P(1)	92.2(3)	91.87(16)	92.0(2)	91.25(17)
O(1)–Re(1)–P(1)	89.8(2)	90.16(13)	85.34(15)	85.79(11)
N(1)–Re(1)–P(1)	90.2(2)	89.96(13)	91.85(19)	91.75(10)
X(1)–Re(1)–P(1)	87.27(9)	87.34(4)	88.84(8)	89.11(4)
O(1)–Re(1)–P(2)	90.2(2)	89.79(13)	88.10(15)	87.57(11)
N(2)–Re(1)–P(2)	87.8(3)	88.18(16)	94.6(2)	95.36(17)
N(1)–Re(1)–P(2)	89.8(2)	90.03(13)	89.97(19)	89.85(10)
P(1)–Re(1)–P(2)	179.96(12)	179.95(6)	172.91(8)	172.90(6)
P(2)–Re(1)–X(1)	92.75(9)	92.66(4)	88.36(8)	88.28(4)
C(32)–N(2)–Re(1)	167.9(8)	170.0(4)	169.0(7)	169.4(5)

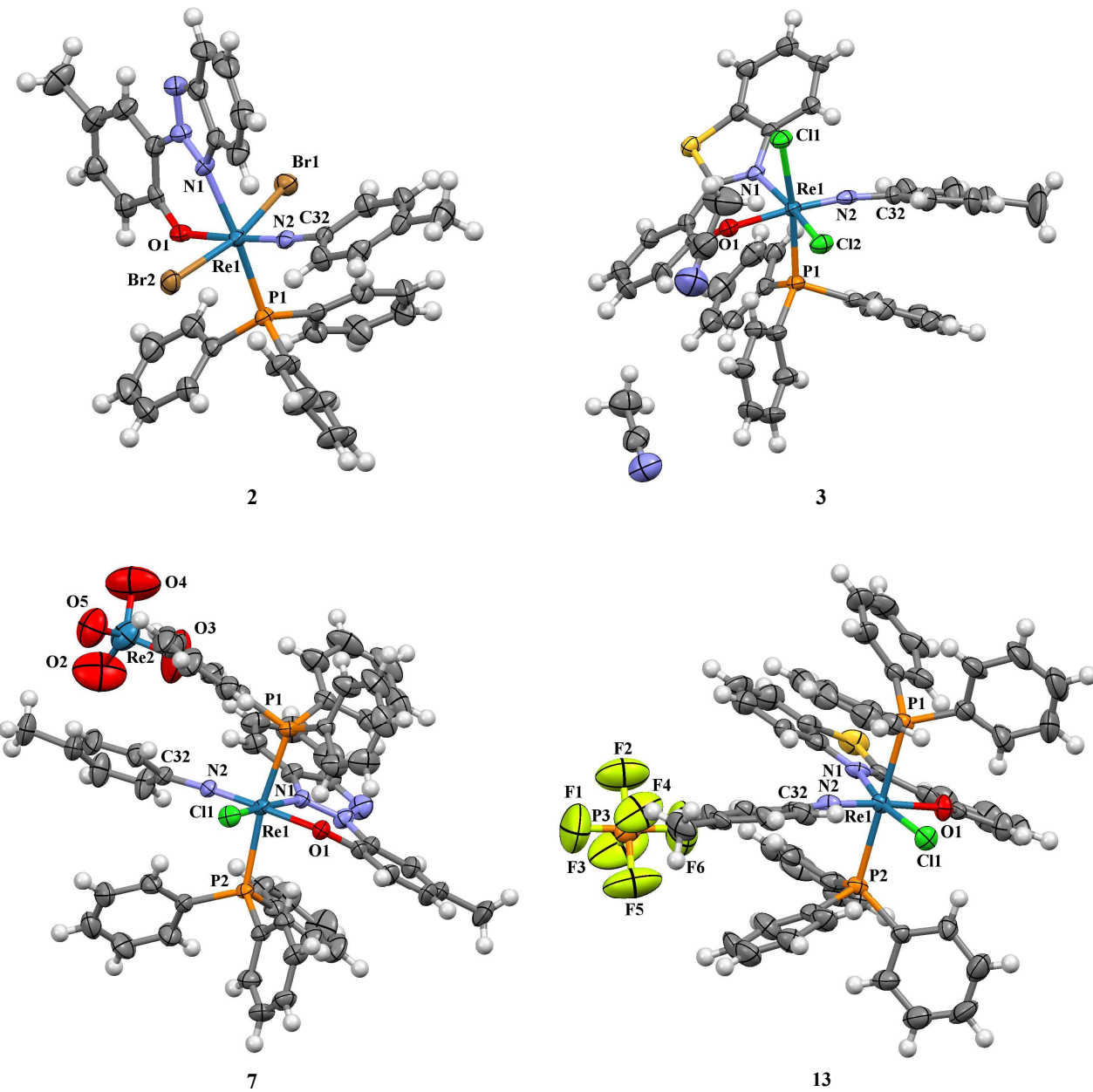


Fig. 1 A perspective view showing the molecular structure of the representative complexes **2**, **3**, **7** and **13**. Displacement ellipsoids are drawn at 50% probability.

Complexes $[\text{Re}(p\text{-NTol})\text{X}_2(\text{L})(\text{PPh}_3)]$ ($\text{X} = \text{Cl}, \text{Br}$; $\text{L} = \text{L}^1, \text{L}^2, \text{L}^3$). The complexes $[\text{Re}(p\text{-NTol})\text{X}_2(\text{L})(\text{PPh}_3)]$ (**1–6**) show a six coordinate rhenium atom with distorted octahedral geometry defined by the *p*-methylphenylimido group, two halide ions, phosphorus atom of PPh_3 molecule and chelating phenolate-based ligand L^1 , L^2 and L^3 . The *p*-methylphenylimido (*p*-NTol) ligand is *trans* to the phenolate oxygen atom, which corresponds to a minimum of *trans* weakening caused by the $\text{Re}=\text{NR}$ multiple bond. Triphenylphosphine molecule with its π - acidity adopts *cis* position with respect to the linear $\text{RN}=\text{Re}-\text{O}$ core and stabilizes it due to accessible π -donation from rhenium to PPh_3 molecule. The repulsion exerted by the $\text{Re}=\text{NR}$ unit is clearly visible in increasing the angles $\text{N}(2)-\text{Re}-\text{N}(1)$, $\text{N}(2)-\text{Re}-\text{X}(1)$ and $\text{N}(2)-\text{Re}-\text{X}(2)$ beyond 90° . The chelating N–O ligand essentially forms a planar six-membered metallacycle with a bite angle $\text{N}(1)-\text{Re}(1)-\text{O}(1)$ of $80.68(7)^\circ$ in **1**, $^{18d} 81.73(13)^\circ$ in **2**, $81.78(18)^\circ$ in **3**, $81.78(11)^\circ$ in **4**, $81.56(8)^\circ$ in **5** and $81.47(14)^\circ$ in **6**.

The halide ions of **1** and **3** are in *cis* relative dispositions, whereas the complexes **2**, **4**, **5** and **6** were found to be *trans*-(X,X) isomers. For both *cis*-(X,X) and *trans*-(X,X) isomers of $[\text{Re}(p\text{-NTol})\text{X}_2(\text{L})(\text{PPh}_3)]$, the $\text{Re}-\text{N}_{\text{imido}}-\text{C}_{\text{imido}}$ bond angle of $175.99(18)^\circ$ in **1**, $^{18d} 174.3(3)^\circ$ in **2**, $170.5(4)^\circ$ in **3**, $174.8(3)^\circ$ in **4**, $172.0(2)^\circ$ in **5** and $172.4(3)^\circ$ in **6** agrees with a linear coordination mode of the arylimido ligands ($167\text{--}176^\circ$), and it is typical of phenyl imido ligands in high oxidation state complexes, in which the metal is relatively electron-deficient and some π -bonding between the imido nitrogen atom and the metal exists.^{18, 19, 22, 23}

The $\text{Re}-\text{N}_{\text{imido}}$ bond lengths of $1.7195(20)\text{ \AA}$ in **1**^{18d}, $1.723(4)\text{ \AA}$ in **2**, $1.704(5)\text{ \AA}$ in **3**, $1.725(3)\text{ \AA}$ in **4**, $1.721(2)\text{ \AA}$ in **5** and $1.722(4)\text{ \AA}$ in **6** fall in the range typical of mononuclear complexes of rhenium(V) having $[\text{Re}=\text{NR}]^{3+}$ core.^{18, 19, 22, 23} The interatomic distances between the rhenium atom and phenolate oxygen atom of $1.9881(17)\text{ \AA}$ in **1**^{18d}, $1.997(3)\text{ \AA}$ in **2**, $2.008(4)\text{ \AA}$ in **3**, $2.016(3)\text{\AA}$ in **4**, $2.0113(18)\text{ \AA}$ in **5** and $2.004(3)\text{ \AA}$ in **6** reflect single bond character,²⁴ indicating only slight electron delocalization in the $\text{RN}=\text{Re}-\text{O}$ unit. A noticeable difference in $\text{Re}-\text{O}(1)$ and $\text{Re}-\text{N}(1)$ of **1–6** can be understood in terms of Pearson's hard-soft acid-base theory. The Re(V) (hard Lewis acid) forms stronger bonds with oxygen (hard base) rather than with the comparatively softer base nitrogen. Except for a slight shortening of $\text{Re}-\text{N}(1)$ in *cis* isomers (**1** and **3**) compared to **2**, **4**, **5** and **6**, no extraordinary differences were noticed in bond lengths between *cis*-(X,X) and *trans*-(X,X) isomers of $[\text{Re}(p\text{-NTol})\text{X}_2(\text{L})(\text{PPh}_3)]$.

Complexes $[\text{Re}(p\text{-NTol})\text{X}(\text{L})(\text{PPh}_3)_2]\text{Z}$ ($\text{X} = \text{Cl}, \text{Br}$; $\text{Z} = \text{ReO}_4^-$, PF_6^-). The cation $[\text{Re}(p\text{-NTol})\text{X}(\text{L})(\text{PPh}_3)_2]^+$ in the compounds **7–16** has a distorted octahedral configuration with two *trans*-located triphenylphosphine molecules, chelating uninegative N,O-donor ligand, halide ion and *p*-methylphenylimido ligand. Likewise in the neutral complexes $[\text{Re}(p\text{-NTol})\text{X}_2(\text{L})(\text{PPh}_3)]$, the oxygen

atom of the chelating ligand occupies *trans* position to the *p*-methylphenylimido ion and the RN=Re–O core with multiply bonded imido ligand is stabilized due to accessible π -donation from rhenium to triphenylphosphine molecule. The Re(1)–N(2)–C(32) bond angle [171.5(3) $^\circ$ in **7**, 171.6(5) $^\circ$ in **8**, 171.3(4) $^\circ$ in **9**, 168.5(3) $^\circ$ in **10**, 167.9(8) $^\circ$ in **13**, 170.0(4) $^\circ$ in **14**, 169.7(5) $^\circ$ in **15** and 169.3(4) $^\circ$ in **16**] indicates a linear coordination mode of the arylimido ligand in the structures.^{19, 20, 23, 24} The Re–N_{imido} bond lengths of **7–10** and **13–16** [1.731(4) Å in **7**, 1.741(5) Å in **8**, 1.722(4) Å in **9**, 1.732(3) Å in **10**, 1.734(8) Å in **13**, 1.717(5) Å in **14**, 1.740(5) Å in **15** and 1.732(4) Å in **16**] confirm the presence of a triple bond Re–N_{imido}.^{18, 19, 22, 23}

Compared to above mentioned [Re(*p*-NTol)X₂(L)(PPh₃)], the interatomic distances between the rhenium atom and the oxygen atom of phenolate-based ligands [1.972(3) Å in **7**, 1.979(4) Å in **8**, 1.983(3) Å in **9**, 1.974(3) Å in **10**, 2.002(7) Å in **13**, 1.984(4) Å in **14**, 1.983(5) Å in **15** and 1.975(3) Å in **16**] are somewhat shorter. A larger delocalization of electron density in the linear RN=Re–O core in **7–16** results in less pronounced electron transfer by π donation from rhenium to triphenylphosphine molecule. The Re–P distances of **7–10** and **13–16** are significantly longer than those found in [Re(*p*-NTol)X₂(L)(PPh₃)] (**1–6**), but similar to other rhenium(V) complexes incorporating two *trans* located phosphine ligands. The average value of Re–PPh₃ bond distance calculated for 35 Re(V) complexes with two PPh₃ in *trans* position to each is 2.480(9) Å.²⁵ The Re–N(1) bond lengths in the [Re(*p*-NTol)X(L)(PPh₃)₂]⁺ of **7–10** and **13–16** well correlate with values reported here for *cis*–(X,X)-[Re(*p*-NTol)X₂(L)(PPh₃)].

IR and ¹H NMR spectra. Characteristic bands attributed to ν(C=N), ν(C=C) stretching modes of the chelating ligand of **1–16** appear in the range 1620–1550 cm^{−1} and they are only slightly shifted with respect to the free ligands.

Intense absorptions associated with the stretching modes of perrhenate ions of [Re(*p*-NTol)X(L)(PPh₃)₂]ReO₄ occur at 905 cm^{−1} for **7**, 908 cm^{−1} for **8**, 909 cm^{−1} for **9** and 903 cm^{−1} for **10**. The IR spectra of the complexes [Re(*p*-NTol)X(L)(PPh₃)₂]PF₆ exhibit a broad band in the range 830–880 cm^{−1} indicative of PF₆ group. For all compounds **1–16**, the ν(Re–NTol) stretches are extremely difficult to identify as these vibrations are mixed with ν_{C=N} and ν_{P-C} modes of PPh₃ and N–O ligands.^{18, 19, 22, 23}

The ¹H NMR spectra of **1–6** confirmed the occurrence of only one isomer in solution. Distinctive signals attributed to the alkyl protons of the *p*-tolylimido group of **2–16** and methyl groups attached to the phenolate ring of *hmpbta* ligand in **2**, **7**, **8**, **11** and **12** occur in the ranges 2.37–2.20 ppm and 2.20–2.09 ppm, respectively. The aromatic region of **2–16** is dominated by signals of triphenylphosphine protons, which partially obscure protons of the arylimido group and chelating ligand. Comparison of the ¹H NMR spectra of [Re(*p*-NTol)X₂(L)(PPh₃)] and [Re(*p*-NTol)X(L)(PPh₃)₂]Z compounds shows evidence of a

downfield shift of the signals of the phenolate-based ligands in the former one. This behaviour indicates stronger interactions between rhenium and chelating ligand in $[Re(p\text{-NTol})X(L)(PPh_3)_2]Z$ compounds. The lack of paramagnetic broadening or shifts of resonances in the 1H NMR spectra confirms diamagnetism of the complexes **2–16**.

The coordination of the phosphine in **2–16** was additionally confirmed by ^{31}P NMR spectroscopy. The single peaks attributed to the coordinated phosphine were observed in the complexes $[Re(p\text{-NTol})X_2(L)(PPh_3)]$ and $[Re(p\text{-NTol})X(L)(PPh_3)_2]Z$ in the range 25.53–26.27 ppm and 25.57–25.65 ppm. As expected, these phosphorous signals are downfield from uncoordinated triphenylphosphine (−6 ppm) and upfield from triphenylphosphine oxide (29.8 ppm).

2.3 Oxidation of alcohols with *tert*-BuOOH catalyzed by certain rhenium complexes

Complexes of various transition metals are well-known catalysts for oxidations of alcohols²⁶ and hydrocarbons^{27,28} with peroxides. We explored the catalytic activity of complexes **11–16** in the oxidation of alcohols and alkanes by aqueous hydrogen peroxide and *tert*-BuOOH (TBHP) under mild conditions. All these rhenium complexes turned out to be almost inactive in oxidation with H_2O_2 (50% aqueous) in acetonitrile at 50–70 °C. We were unable to oxidize benzene under the same conditions using either hydrogen peroxide or TBHP. In contrast, certain complexes exhibited high activity in oxidation of alcohols with TBHP. It is noteworthy that only two compounds, **13** and **14**, are efficient catalysts in the oxidation of 1-phenylethanol to acetophenone:



Activity of complexes **15** and **16** is lower, whereas in the presence of compounds **11** and **12** the rate of 1-phenylethanol oxidation is equal to that in the absence of any catalyst. Concentrations of acetophenone after 1 h and the initial reaction rates $W_0 = d[\text{PhC(=O)CH}_3]/dt$ are summarized in Table 7.

Table 7 Comparison of complexes **11–16** as catalyst in the oxidation of 1-phenylethanol to acetophenone ^a

Entry	Catalyst	Concentration of PhC(=O)CH ₃ , M	Rate 10 ⁵ × d[PhC(=O)CH ₃]/dt, M s ⁻¹
1	13	0.06	1.7
2	14	0.014	0.38
3	15	0.009	0.25
4	16	0.008	0.22
5	11	0.007	0.20
6	12	0.003	0.008
7	None	0.003	0.008

^a Conditions. Catalyst concentration, 1 × 10⁻³ M; 1-phenylethanol, 0.36 M; TBHP (70% aqueous) 1.67 M; 1 h at 70 °C.

Oxidation properties of complex **13** were studied in more detail. The oxidation of 1-phenylethanol to produce acetophenone with TBHP catalyzed by compound **13** is presented in Fig. 2. Yield of acetophenone is 80% based on the initial 1-phenylethanol, TON attained 290 after 30 h and initial TOF was 60 h⁻¹.

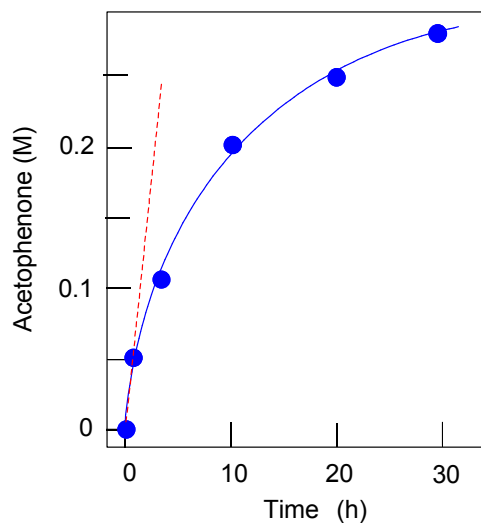


Fig. 2 Accumulation of acetophenone in the oxidation of 1-phenylethanol (0.36 M) with TBHP (1.67 M) catalyzed by compound **13** (1×10^{-3} M) in acetonitrile solution at 70 °C. The initial rate W_0 was determined from the slope of the tangent (in an example shown as dotted straight line) to the kinetic curve of acetophenone accumulation.

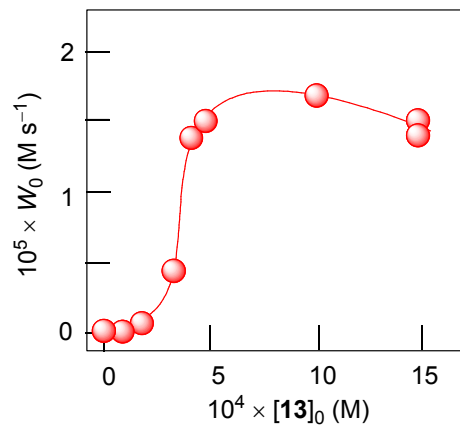


Fig. 3 Dependence of the initial oxidation rate W_0 on initial concentration of compound **13** in the oxidation of 1-phenylethanol (initial concentration 0.36 M) with TBHP (initial concentration 1.67 M) at 70 °C in acetonitrile solution catalyzed by compound **13**.

The dependence of initial reaction rate W_0 on the initial concentration of catalyst **13** is shown in Fig. 3. It can be seen that this dependence is of a sigmoid-type that is at $[13]_0 \leq 5 \times 10^{-4}$ M the order of the reaction rate relative to **13** is higher than first order.

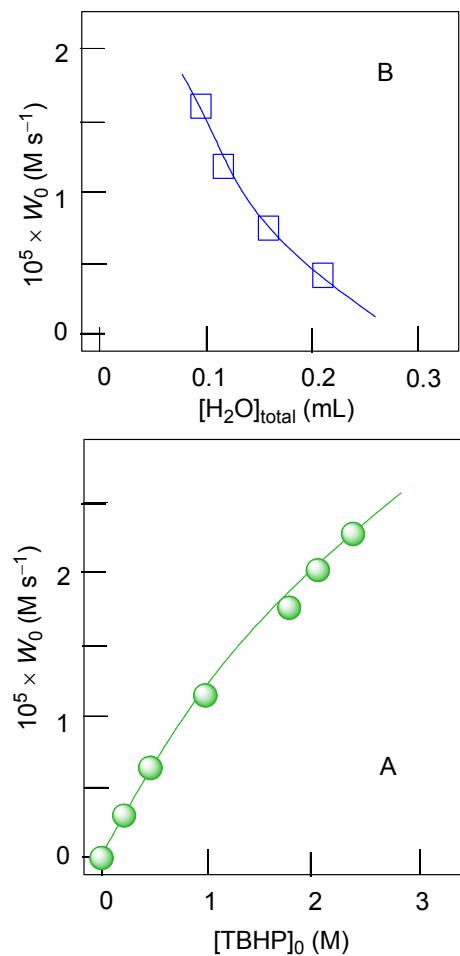
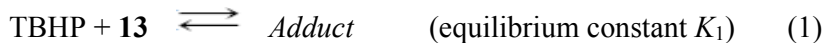
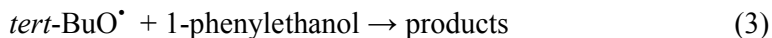


Fig. 4 Graph A: dependence of the initial oxidation rate W_0 on initial concentration of TBHP in the oxidation of 1-phenylethanol (initial concentration 0.25 M) with TBHP (at fixed water concentration) catalyzed by compound **13** (1×10^{-3} M) at 70 °C in acetonitrile solution. Graph B: effect of water on the initial rate.

Dependences of initial rates on initial concentrations of TBHP and 1-phenylethanol are presented in Figs. 4 and 5, respectively. Experiments with different concentrations of TBHP were carried out at fixed total concentration of water. The mode of dependence of W_0 on the initial concentration of TBHP indicates²⁹ the formation of an intermediate adduct between the catalyst **13** and TBHP followed by subsequent decomposition of the adduct to generate an intermediate species *tert*-BuO[·] which induces the alcohol oxidation:



The dependence mode of the initial oxidation rate on 1-phenylethanol concentration reflects²⁹ a competition between the alcohol and solvent acetonitrile for the interaction with the oxidizing species *tert*-BuO[•] generated in reaction (2):



In quasi-stationary approach relative concentration of *tert*-BuO[•] we can obtain expression (5) for the initial oxidation rate:

$$\frac{d[\text{PhCH(OH)CH}_3]}{dt} = W_0 = \frac{W_2}{1 + \frac{k_4[\text{CH}_3\text{CN}]}{k_5[\text{PhCH(OH)CH}_3]_0}} \quad (5)$$

where W_2 is the rate of reaction (2).

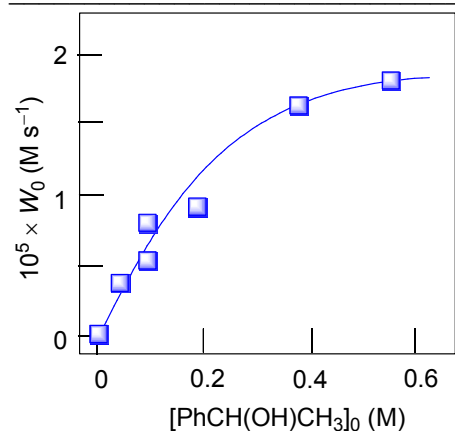


Fig. 5 Dependence of the initial oxidation rate W_0 on initial concentration of 1-phenylethanol in the oxidation of 1-phenylethanol with TBHP (initial concentration 1.67 M) catalyzed by compound **13** (1×10^{-3} M) at 70 °C in acetonitrile solution.

Aliphatic alcohols, both cyclic (cyclooctanol) and linear (2-octanol) ones, can be also transformed into the corresponding ketones in the reaction with the TBHP/**13** system. Some examples are presented in Figs. 6 and 7. The yield of cyclooctanone attained 88% after 14 h (Fig. 6, curve 3). In the presence of

nitric acid the oxidation is slower (compare Fig. 6, curves 1 and 2). Linear 2-octanol is transformed into 2-octanone. Compounds **11**, **12** and **14** are less efficient catalysts (Fig. 8).

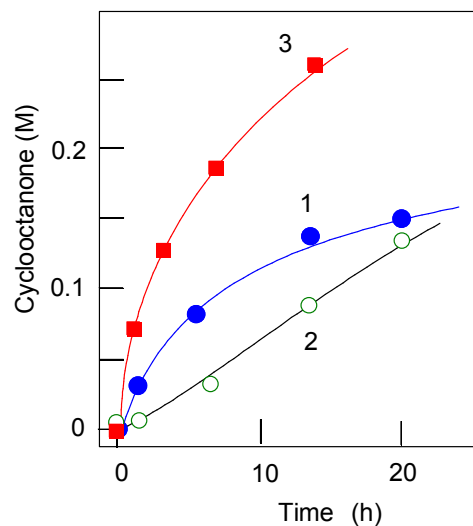


Fig. 6 Accumulation of cyclooctanone in the oxidation of cyclooctanol with TBHP (1.67 M) catalyzed by compound **13** in acetonitrile solution. Conditions. $[13]_0 = 2 \times 10^{-3}$ M, $[\text{cyclooctanol}]_0 = 0.6$ M, 60 °C (curve 1); 1×10^{-3} M, $[\text{cyclooctanol}]_0 = 0.6$ M, $[\text{HNO}_3]_{\text{added}} = 0.05$ M, 60 °C (curve 2); $[13]_0 = 1 \times 10^{-3}$ M, $[\text{cyclooctanol}]_0 = 0.3$ M, 70 °C (curve 3). Yield of cyclooctanone is 88% after 14 h.

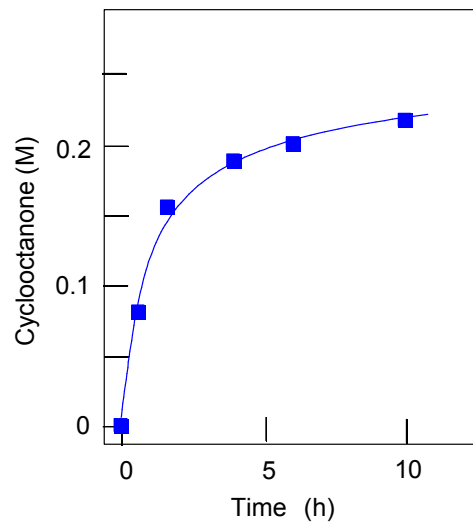


Fig. 7 Accumulation of 2-octanone in the oxidation of 2-octanol (0.6 M) with TBHP (1.67 M) catalyzed by compound **13** (1×10^{-3} M) in acetonitrile solution. at 60 °C .

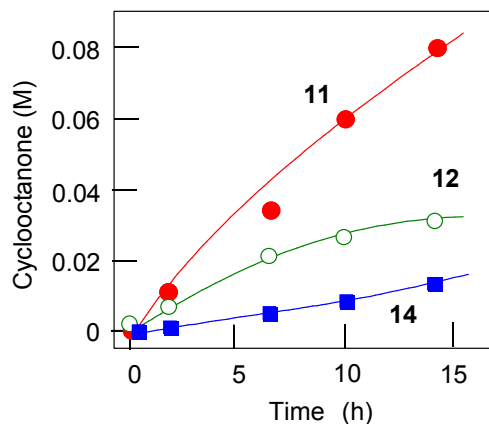


Fig. 8 Accumulation of cyclooctanone in the oxidation of cyclooctanol (0.3 M) with TBHP (1.67 M) in acetonitrile solution catalyzed by compounds (1×10^{-3} M) **11** (60 °C), **12** (70 °C) and **14** (60 °C).

2.4 Catalytic oxidation of alkanes with *tert*-BuOOH

Many works have been devoted to the oxygenation of alkanes with peroxides, particularly, with TBHP.^{30,31} The oxygenation of saturated hydrocarbons as well as of some alkane derivatives usually gives rise to the formation of the corresponding alkyl hydroperoxide, ROOH, as the main primary product. To demonstrate the formation of alkyl hydroperoxide in this oxidation and to estimate its concentration in the course of the reaction we used a simple method developed earlier by one of us.³² If an excess of solid PPh₃ is added to the sample of the reaction solution before the GC analysis, the alkyl hydroperoxide present is completely reduced to the corresponding alcohol. Comparing measured by the GC concentrations of the alcohol and ketone before and after reduction with PPh₃ we can estimate the real concentrations of the three products (alkyl hydroperoxide, ketone and alcohol) present in the reaction solution. In many experiments we determined concentrations of isomers only after reduction with PPh₃.

Complexes **11–16** turned out to be less efficient in oxidation of alkanes in comparison with their activity as catalysts for the alcohol oxidation. Turnover numbers attained only 20–30 after 2–4 h. In order to determine the nature of the alkane oxidizing species we measured the selectivity parameters in oxidations of certain alkanes with TBHP catalyzed by compounds **11–16**. These values for the oxidation of linear heptane and octane (Table 8, entries 1–8) can be compared with the parameters determined previously³³ for other systems which are also given in Table 8 for comparison. These parameters are slightly higher in comparison with the selectivities determined previously for the systems generating free hydroxyl radicals (entries 9–24) and they are comparable with parameters obtained for other metal-catalyzed oxidations with TBHP (entries 25 and 26). Enhanced selectivities in experiments reflected by entries 27 and 28 (as well as 20) can be due to sterical hindrance. Careful examination selectivity

parameters for the oxidation with TBHP catalyzed rhenium complexes prepared in this work, especially, reflected in entries 4 and 5 show enhanced reactivity C–H bonds in position 2. Similar situation, although more strongly pronounced, was found in the profiles for oxidation with catalysts containing sterically hindered reaction centers (compare profiles presented in Fig. S5).

Table 8 Regioselectivity parameters for oxidation of *n*-heptane or *n*-octane with TBHP or H₂O₂ catalyzed by complexes prepared in this work and (for comparison) by certain other systems ^a

Entry	System	Alkane	TON	C(1):C(2):C(3):C(4)	Ref.
1	11 -TBHP	Heptane	20	1 : 7.5 : 5.0 : 3.3	This work
2	12 -TBHP	Heptane	20	1 : 8.3 : 6.3 : 6.0	This work
3	13 -TBHP	Heptane	22	1 : 13.2 : 8.8 : 5.9	This work
4	13 -TBHP	Octane (no HNO ₃)	16	1 : 6.8 : 3.6 : 2.8	This work
5	13 -TBHP	Octane (with HNO ₃)	23	1 : 3.8 : 1.9 : 1.5	This work
6	14 -TBHP	Heptane	20	1 : 8.2 : 5.4 : 5.0	This work
7	15 -TBHP	Heptane	19	1 : 8.5 : 6.5 : 5.0	This work
8	16 -TBHP	Heptane	13	1 : 9.1 : 5.3 : 4.4	This work
9	hv/H ₂ O ₂	Heptane		1 : 7.0 : 6.0 : 7.0	33a
10	(<i>n</i> -Bu ₄ N)VO ₃ /PCA/H ₂ O ₂	Heptane		1 : 9.0 : 7.0 : 7.0	33a-c
11	[(η^6 - <i>p</i> -cym)OsCl ₂] ₂ /py/H ₂ O ₂	Octane		1 : 2.8 : 2.8 : 2.6	33d
12	(η^6 - <i>p</i> -cym)Os(py)Cl ₂ /py/H ₂ O ₂	Octane		1.0 : 4.7 : 4.8 : 4.3	33e
13	Os ₃ (CO) ₁₂ /py/H ₂ O ₂	Octane		1 : 4.0 : 4.0 : 4.0	10f,33f
14	“Os”/H ₂ O ₂	Heptane		1 : 5.5 : 5.0 : 4.5	33g
15	Cp* ₂ Os/py/H ₂ O ₂	Heptane		1 : 7.0 : 7.0 : 7.0	33h
16	FeSO ₄ /H ₂ O ₂	Heptane		1 : 5.0 : 5.0 : 4.5	33a,i
17	Fe ₂ (HPTB)/PCA/H ₂ O ₂	Heptane		1 : 6.0 : 6.0 : 5.0	33j
18	“Fe-S-Fe”/PCA/py/H ₂ O ₂	Heptane		1:6.5:6.5:6	33k
19	“Fe ₂ ”/H ₂ O ₂	Heptane		1 : 10.0 : 10.0 : 6.0	33l
20	“Fe ₄ ”/H ₂ O ₂	Heptane		1 : 15.0 : 14.0 : 11.0	33l
21	“Re-ind”/H ₂ O ₂	Octane		1 : 6.0 : 6.0 : 5.0	18a
22	Al(NO ₃) ₃ /H ₂ O ₂	Heptane		1 : 5.3 : 5.4 : 4.9	33m
23	Al(NO ₃) ₃ /H ₂ O ₂	Octane		1 : 5.6 : 5.6 : 5.0	33m
24	Bi(NO ₃) ₃ /HNO ₃ /H ₂ O ₂	Octane		1.0 : 4.4 : 4.3 : 4.0	33n
25	Cu(H ₃ L ³)(NCS)/TBHP	Octane		1 : 12.0 : 8.0 : 7.0	33o
25	“Cu ₄ -O-Si”/TBHP	Octane		1 : 10.5 : 8.2 : 7.0	33p
27	“Cu ₄ -N”/TBHP	Heptane		1 : 34 : 23 : 21	33q
28	“Cu ₄ -N”/TBHP	Octane		1 : 65 : 32 : 30	33q

^a Parameters C(1):C(2):C(3):C(4) are relative normalized reactivities of H atoms at carbon atoms C(1), C(2), C(3) and C(4) of *n*-heptane or *n*-octane chain. All parameters were measured after reduction of the reaction mixtures with PPh₃ before GC analysis and calculated based on the ratios of isomeric alcohols.

^b Abbreviations. Symbol hν means UV irradiation. PCA is pyrazine-2-carboxylic acid. π-*p*-cym is *p*-cymene. Cp*₂O_s is decamethyllosmocene. “Os” is complex (2,3-η-1,4-diphenylbut-2-en-1,4-dione)undecacarbonyl triangulotriosmium. Fe₂(HPTB) is complex [Fe₂(HPTB)(μ-OH)(NO₃)₂](NO₃)₂, HPTB = N,N,N',N'-tetrakis(2-benzimidazolylmethyl)-2-hydroxo-1,3-diaminopropane. “Fe-S-Fe” is (OC)₃Fe(μ-PhS)₂Fe(CO)₃. “Fe₂” is binuclear complex [Fe₂(N₃O-L¹)₂(μ-O)(μ-OOCCH₃)]⁺, where L¹ = 1-carboxymethyl-4,7-dimethyl-1,4,7-triazacyclononane. “Fe₄” is tetranuclear complex [Fe₄(N₃O₂-L)₄(μ-O)₂]⁴⁺ with ligand N₃O₂-L¹. Complex “Re-ind” is *cis*-(Cl,Cl)-[Re(*p*-NC₆H₄CH₃)Cl₂(ind-3-COO)(PPh₃)]·2MeOH (where ind-3-COOH is indazole-3-carboxylic acid). In the complex Cu(H₃L³)(NCS), ligand H₄L³ is N,N,N',N'-tetrakis-(2-hydroxyethyl)ethylenediamine. “Cu₄-O-Si” is [(PhSiO_{1.5})₁₂(CuO)₄(NaO_{0.5})₄]. “Cu₄-N” is tetracopper(II) triethanolamine complex [O<Cu₄{N(CH₂CH₂O)₃}₄(BOH)₄][BF₄]₂.

The oxidation with TBHP catalyzed by the rhenium complexes of *cis*-1,2-DMCH and *trans*-1,2-DMCH (where DMCH is dimethylcyclohexane) proceeds non-stereoselectively. Thus, parameter *trans/cis* for the oxidation of *cis*-1,2-DMCH catalyzed by **12** was 0.8 and for *trans*-1,2-DMCH it was 0.75. For the catalysis by **13** in the case of *cis*-1,2-DMCH *trans/cis* was 0.7. Thus, we can conclude that selectivity parameters testify that in the main pathway alkanes are oxidized by the systems under discussion with the participation of *tert*-butoxyl radicals.

The oxygenation of methylcyclohexane (MCH) proceeds mainly at the tertiary carbon atom with formation of 1-methylcyclohexanol after reduction with PPh₃ (product **P5**; see the ESI, Figs. S5a and S5b). It should be noted that in the oxidation with TBHP catalyzed by complex **13** (Fig. S5bA) as well as oxidation with H₂O₂ catalyzed by complex *cis*-(Cl,Cl)-[Re(*p*-NC₆H₄CH₃)Cl₂(ind-3-COO)(PPh₃)]·2MeOH (Fig. S5bB) the position 2 (products **P6** and **P7**) relative to the methyl group of the substrate is less reactive than the corresponding positions 3 (**P8** and **P10**) and 4 (**P9** and **P11**) comparing the formation of isomeric alcohols. This can be explained by some sterical hindrance which is apparently due to the involvement of a bulky oxidizing species. Indeed, products **P6** and **P7** are formed in relatively high concentration in the oxidations with H₂O₂ catalyzed by the osmium complexes (Fig. S5bK,L) and bismuth salt (Fig. S5bJ). At the same time concentration of isomers **P6** and **P7** in the reactions with TBHP catalyzed by bulky catalysts (Fig. S5bD,E,G) are low.

3. Conclusions

The reactivity of $[\text{Re}(p\text{-NTol})\text{X}_3(\text{PPh}_3)_2]$ ($\text{X} = \text{Cl}, \text{Br}$) towards phenolate-based chelating ligands (2-(2-hydroxy-5-methylphenyl)benzotriazole, 2-(2-hydroxyphenyl)benzothiazole, and 2-(2-hydroxyphenyl)benzoxazole) has been examined and compared with the related exchange reactions performed with carboxylate-based N,O-donor ligands. As a result of these studies, 15 novel rhenium(V) imidocomplexes have been obtained and characterized structurally and spectroscopically. The findings enhance our understanding of the structural preferences of the imido rhenium(V) complexes with uninegative N,O-donor ligands. Different tested complexes exhibited different catalytic activities in oxidation of alcohols and alkanes with TBHP in acetonitrile. Experiments with methylcyclohexane led to a conclusion that some sterical hindrance exists around the reaction center.

4. Experimental

4.1 Materials

All chemicals and bidentate ligands were purchased from commercial sources and were used without further purification. The complexes *mer*- $[\text{Re}(p\text{-NTol})\text{X}_3(\text{PPh}_3)_2]$ ($\text{X} = \text{Cl}, \text{Br}$) were prepared according to the literature methods.³⁴

4.2 Instrumentation

IR spectra were recorded on a Nicolet iS5 spectrophotometer in the spectral range 4000–400 cm⁻¹ with the samples in form of KBr pellets. The ¹H NMR, ¹³C NMR and ³¹P NMR spectra were recorded (298 K) on Bruker Avance 500 NMR spectrometer at a resonance frequency of 500 MHz for ¹H NMR spectra, 125 MHz for ¹³C NMR spectra and 162 MHz for ³¹P NMR using DMSO-d₆ or CDCl₃ as solvent and TMS as an internal solvent. The X-ray intensity data of **2–16** were collected on a Gemini A Ultra diffractometer equipped with Atlas CCD detector and graphite monochromated MoK_α radiation ($\lambda = 0.71073 \text{\AA}$) at room temperature. Details concerning crystal data and refinement are given in Table 1. Lorentz, polarization and empirical absorption correction using spherical harmonics implemented in SCALE3 ABSPACK scaling algorithm were applied.³⁵ The structures were solved by the Patterson method and refined by full-matrix least-squares on F^2 using SHELXL97.³⁶ All the non-hydrogen atoms were refined anisotropically using full-matrix, least-squares technique. The hydrogen atoms were treated as „riding” on their parent carbon atoms and assigned isotropic temperature factors equal 1.2 (non-methyl) and 1.5 (methyl) times the value of equivalent temperature factor of the parent atom. The methyl groups were allowed to rotate about their local threefold axis. Largest residual electron density in the examined structures is located close to the heavy atoms. In the compounds **15** and **16**, the carbon atoms of one phenyl ring of the

triphenylphosphine molecule and the fluorine anions of hexafluorophosphate show symptoms of disorder, exhibiting in the revolution (prolation and oblation) of the anisotropic displacement ellipsoids.

CCDC- 1422185 (for **2**), - 1422179 (for **3**), - 1422180 (for **4**), - 1422176 (for **5**), - 1422182 (for **6**), - 1422178 (for **7**), - 1422177 (for **8**), - 1422183 (for **9**), - 1422181 (for **10**), - 1422188 (for **13**), - 1422187 (for **14**), - 1422186 (for **15**) and - 1422184 (for **16**) contain the supplementary crystallographic data for this paper. These data can be obtained free of charge from The Cambridge Crystallographic Data Centre via www.ccdc.cam.ac.uk/data_request/cif.

4.3 Preparation of complexes **2–6**

mer-[Re(*p*-NTol)X₃(PPh₃)₂] (0.54 mmol) was added to the corresponding phenolate-based ligand (0.60 mmol) in acetonitrile (60 mL) and the reaction mixture was refluxed for 4 h. The resulting solution was reduced in volume to 10 mL and allowed to cool to room temperature. A crystalline precipitate of compound **2–6** was filtered off and dried in the air. X-ray quality brown crystals of **2–6** were obtained by slow recrystallization from acetonitrile.

trans-(Br,Br)-[Re(*p*-NTol)Br₂(L¹)(PPh₃)] (2). (0.52 g of [Re(*p*-NTol)Br₃(PPh₃)₂] and 0.13 g of 2-(2-hydroxy-5-methylphenyl)benzotriazole yielded to 370 mg of **2**; yield 80%). C₃₈H₃₂Br₂N₄OPRe (937.67 g/mol): calcd. C 48.67, H 3.44, N 5.97 %; found C 48.37, H 3.32, N 5.69 %. IR (KBr; v/cm⁻¹): 3055(w), 1610(w), 1587(w), 1503(s), 1496(s), 1481(sh), 1432(m), 1349(w), 1336(w), 1311(m), 1295(w), 1274(w), 1260(m), 1207(w), 1187(w), 1171(w), 1132(w), 1090(w), 1074(sh), 1028(w), 1012(w), 997(w), 904(w), 836(sh), 824(s), 784(w), 744(s), 705(sh), 691(s), 638(w), 616(m), 557(w), 528(vs), 499(m) and 458(w).

¹H NMR (DMSO, ppm): δ = 8.04(d, 1H, 8.8Hz), 7.62(dd, 4H, 11.5, 7.2Hz), 7.59 – 7.50(m, 3H), 7.47(t, 2H), 7.39(s, 4H), 7.29(dd, 11H, 19.9, 8.5Hz), 7.08 – 6.99(m, 1H), 2.32(s, 3H) and 2.20(s, 3H).

¹³C NMR (125 MHz, DMSO-d₆): δ = 148.5, 143.7, 141.8, 133.8, 133.7, 133.6, 133.2, 132.5, 132.4, 131.9, 131.8, 129.5, 129.2, 129.0, 127.9, 124.5, 120.1, 118.2, 117.4, 20.7, 20.4 ppm.

³¹P NMR (DMSO-d₆): δ = 26.08 ppm.

cis-(Cl,Cl)-[Re(*p*-NTol)Cl₂(L²)(PPh₃)]·2MeCN (3). (0.43 g of [Re(*p*-NTol)Cl₃(PPh₃)₂] and 0.14 g of 2-(2-hydroxyphenyl)benzothiazole yielded to 347 mg of **3**; yield 80%). C₄₂H₃₆Cl₂N₄OSPRe (932.88 g/mol): calcd. C 54.07, H 3.89, N 6.01%; found C 54.42, H 3.78, N 5.89 %. IR (KBr; v/cm⁻¹): 3060(w), 1592(w), 1572(w), 1481(m), 1472(sh), 1454(sh), 1434(s), 1328(w), 1287(w), 1268(w), 1253(sh),

1231(w), 1192(w), 1170(w), 1127(sh), 1089(m), 1073(sh), 1029(w), 1016(w), 998(w), 842(w), 822(m), 745(s), 703(sh), 694(vs), 650(sh), 618(w), 573(w), 561(w), 520(vs), 508(s), 494(m), 458(w) and 445(w).

¹H NMR (DMSO, ppm): δ = 8.61(d, 1H, 9.0Hz), 8.25 – 8.18(m, 1H), 7.92(d, 1H, 7.7Hz), 7.73 – 7.65(m, 5H), 7.53(dd, 10H, 14.4, 6.0Hz), 7.43(d, 3H, 8.3Hz), 7.24(t, 1H, 7.7Hz), 7.04(d, 3H, 8.3Hz), 6.95(t, 1H, 7.3Hz), 5.89(d, 1H, 8.0Hz), 2.68(s, 3H), 2.33(s, 3H) and 2.16(s, 3H).

¹³C NMR (125 MHz, DMSO-d₆): δ = 153.0, 151.5, 138.2, 134.0, 133.9, 133.3, 132.5, 131.9, 130.9, 130.5, 129.7, 129.2, 129.0, 128.7, 128.6, 127.6, 124.7, 123.5, 122.8, 121.4, 119.2, 118.5, 21.9 ppm.

³¹P NMR (DMSO-d₆): δ = 25.90 ppm.

trans-(Br,Br)-[Re(p-NTol)Br₂(L²)(PPh₃)] (4). (0.52 g of [Re(p-NTol)Br₃(PPh₃)₂] and 0.14 g of 2-(2-hydroxyphenyl)benzothiazole yielded to 347 mg of **4**; yield 75%). C₃₈H₃₀Br₂N₂OPSRe (939.69 g/mol): calcd. C 48.57, H 3.22, N 2.98 %; found C 48.71, H 3.29, N 2.83 %.

IR (KBr; v/cm⁻¹): 3059(w), 1593(w), 1553(w), 1479(sh), 1471(s), 1453(sh), 1444(sh), 1433(m), 1413(w), 1350(w), 1327(w), 1290(w), 1276(w), 1220(w), 1187(w), 1172(w), 1150(w), 1126(w), 1101(sh), 1089(w), 1072(sh), 1027(w), 1014(w), 997(w), 984(sh), 955(w), 891(w), 845(w), 824(w), 759(sh), 747(s), 729(sh), 717(sh), 693(s), 622(m), 572(w), 563(sh), 528(vs), 499(m) and 459(w).

¹H NMR (CDCl₃, ppm): δ = 8.68(d, 1H, 8.3Hz), 7.97 – 7.76(m, 8H), 7.48 – 7.31(m, 13H), 7.19(t, 1H, 7.6Hz), 6.90(d, 3H, 7.8Hz), 6.05(d, 1H, 8.1Hz) and 2.21(s, 3H).

³¹P NMR (CDCl₃): δ = 26.27 ppm.

¹³C NMR spectrum of **4** was not recorded due to its low solubility in deuterated solvents.

trans-(Cl,Cl)-[Re(p-NTol)Cl₂(L³)(PPh₃)] (5). (0.43 g of [Re(p-NTol)Cl₃(PPh₃)₂] and 0.13 g of 2-(2-hydroxyphenyl)benzoxazole yielded to 347 mg of **5**; yield 80%). C₃₈H₃₀Cl₂N₂O₂PRE (834.71 g/mol): calcd. C 54.68, H 3.62, N 3.36 %; found C 54.83, H 3.57, N 3.49 %.

IR (KBr; v/cm⁻¹): 3058(w), 1607(m), 1592(m), 1560(w), 1534(m), 1473(vs), 1458(sh), 1432(s), 1352(w), 1334(w), 1315(s), 1261(s), 1249(sh), 1187(w), 1171(w), 1153(w), 1130(w), 1101(sh), 1092(m), 1068(w), 1030(w), 1015(w), 997(w), 873(m), 855(sh), 824(w), 809(w), 758(sh), 751(sh), 742(vs), 692(s), 669(sh), 620(m), 560(w), 529(vs), 500(m), 486(sh), 474(sh), 458(sh), 441(w), 426(w).

¹H NMR (CDCl₃, ppm): δ = 8.08(d, 1H, 8.0Hz), 7.90-7.81(m, 6H), 7.78(d, 1H, 8.2Hz), 7.63(d, 1H, 8.0Hz), 7.48-7.34(m, 12H), 7.22(dd, 2H, 14.5; 7.2Hz), 6.96(d, 3H, 8.0Hz), 6.20(d, 1H, 8.4Hz), 2.26(s, 3H).

¹³C NMR (125 MHz, CDCl₃): δ = 164.7, 155.5, 149.3, 135.4, 135.0, 134.9, 130.6, 129.9, 128.0, 127.9, 125.7, 125.6, 122.9, 119.4, 111.2, 22.1 ppm.

³¹P NMR (CDCl₃): δ = 26.07 ppm.

trans-(Br,Br)-[Re(*p*-NTol)Br₂(L³)(PPh₃)] (**6**). (0.52 g of [Re(*p*-NTol)Br₃(PPh₃)₂] and 0.13 g of 2-(2-hydroxyphenyl)benzoxazole yielded to 370 mg of **6**; yield 80%). C₃₈H₃₀Br₂N₂O₂PR_e (923.63 g/mol): calcd. C 49.41, H 3.27, N 3.03%; found C 49.32, H 3.39, N 3.19 %.

IR (KBr; v/cm⁻¹): 3057(w), 1607(m), 1592(m), 1561(w), 1534(m), 1473(vs), 1458(sh), 1432(s), 1352(w), 1314(s), 1259(s), 1249(sh), 1187(w), 1172(w), 1152(w), 1099(m), 1091(sh), 1070(w), 1030(w), 1015(w), 873(m), 824(w), 809(w), 798(w), 757(sh), 750(sh), 743(vs), 692(s), 669(w), 621(m), 560(w), 528(vs) and 501(m).

¹H NMR (CDCl₃, ppm): δ = 8.08(t, 1H, 9.1Hz), 7.93 – 7.83(m, 4H), 7.77 – 7.56(m, 5H), 7.56 – 7.36(m, 13H), 7.25 – 7.12(m, 2H), 7.06 – 6.93(m, 2H) and 2.28(s, 3H).

³¹P NMR (CDCl₃-d₆): δ = 26.27 ppm.

¹³C NMR spectrum of **4** was not recorded due to its low solubility in deuterated solvents.

4.4 Preparation of complexes 7–10

Compound *mer*-[Re(*p*-NTol)X₃(PPh₃)₂] (0.54 mmol) was added to the corresponding phenolate-based ligand (0.60 mmol) in methanol (60 mL) and the reaction mixture was refluxed for 4 h. The resulting solution was allowed to evaporate slowly at room temperature. A brown crystalline precipitate of **7–10** was filtered off and dried in the air. X-ray quality brown crystals of **7–9** were obtained by slow recrystallization from methanol.

[Re(*p*-NTol)Cl(L¹)(PPh₃)₂]·ReO₄ (**7**). (0.43 g of [Re(*p*-NTol)Cl₃(PPh₃)₂] and 0.13 g of 2-(2-hydroxy-5-methylphenyl)benzotriazole yielded to 370 mg of **7**; yield 60%). C₅₆H₄₇ClN₄O₅P₂Re₂ (1325.77): calcd. C 50.73, H 3.57, N 4.23 %; found C 50.91, H 3.44, N 4.39 %. IR (KBr; v/cm⁻¹): 3052(w), 1590(w), 1572(w), 1503(m), 1497(sh), 1481(w), 1435(m), 1335(w), 1300(w), 1264(w), 1251(sh), 1212(w), 1195(w), 1176(w), 1161(w), 1133(w), 1091(m), 1071(sh), 1021(w), 997(w), 973(w), 905(vs), 837(m), 824(sh), 802(w), 786(w), 745(s), 693(s), 651(sh), 638(w), 615(w), 558(w), 537(sh), 518(sh), 512(s), 496(sh), 485(sh) and 447(w).

¹H NMR (DMSO, ppm): δ = 7.91(d, 1H, 8.7Hz), 7.63(t, 1H, 7.4Hz), 7.38-7.28(m, 8H), 7.25-7.15(m, 25H), 7.11-7.05(m, 2H), 6.90(d, 2H, 8.2Hz), 6.68(d, 2H, 8.2Hz), 2.31(s, 3H), 2.16(s, 3H).

¹³C NMR (125 MHz, DMSO-d₆): δ = 151.0, 148.6, 148.4, 143.7, 143.6, 142.4, 142.3, 133.7, 133.6, 133.3, 132.5, 131.9, 131.5, 129.7, 129.1, 129.0, 128.0, 127.8, 127.7, 127.4, 124.5, 122.3, 121.9, 120.1, 118.4, 118.2, 115.7, 20.5, 20.4 ppm.

³¹P NMR (DMSO-d₆): δ = 25.76 ppm.

[Re(*p*-NTol)Br(L¹)(PPh₃)₂]ReO₄ (8). (0.52 g of [Re(*p*-NTol)Br₃(PPh₃)₂] and 0.13 g of 2-(2-hydroxy-5-methylphenyl)benzotriazole yielded to 410 mg of **8**; yield 60%). C₅₆H₄₉BrN₄O₆P₂Re₂ (1388.24): calcd. C 48.45, H 3.56, N 4.04 %; found C 48.64, H 3.61, N 4.12 %. IR (KBr; ν/cm^{-1}): 3053(w), 1590(w), 1571(sh), 1503(m), 1496(m), 1481(sh), 1434(m), 1334(w), 1310(w), 1298(w), 1264(m), 1251(sh), 1209(w), 1196(w), 1176(w), 1160(w), 1135(w), 1090(m), 1072(sh), 1018(w), 997(w), 908(vs), 904(vs), 836(m), 824(sh), 785(w), 763(sh), 743(s), 694(s), 651(w), 638(w), 614(m), 568(sh), 558(w), 536(sh), 528(sh) 518(s), 512(sh), 496(sh), 487(sh), 474(sh), 458(w) and 446(w).

¹H NMR (CDCl₃, ppm): δ = 7.91(d, 1H, 8.6Hz), 7.67 – 7.61(m, 1H), 7.42 – 7.31(m, 8H), 7.27 – 7.09(m, 27H), 6.87(d, 2H, 8.2Hz), 6.65(d, 2H, 8.2Hz), 2.32(s, 3H) and 2.17(s, 3H).

¹³C NMR (125 MHz, DMSO-d₆): δ = 151.0, 148.0, 143.9, 142.4, 142.3, 133.8, 133.7, 133.1, 132.5, 131.6, 131.0, 129.8, 129.3, 129.2, 129.0, 128.3, 128.0, 127.9, 127.2, 125.9, 122.3, 120.3, 115.6, 22.1, 20.5.

³¹P NMR (CDCl₃-d₆): δ = 25.71 ppm.

[Re(*p*-NTol)Cl(L²)(PPh₃)₂]ReO₄ (9). (0.43 g of [Re(*p*-NTol)Cl₃(PPh₃)₂] and 0.14 g of 2-(2-hydroxyphenyl)benzothiazole yielded to 370 mg of **9**; yield 60%). C₅₆H₄₅ClN₂O₅P₂SRe₂ (1327.79): calcd. C 50.65, H 3.42, N 2.11 %; found C 50.82, H 3.35, N 2.18 %.

IR (KBr; ν/cm^{-1}): 3058(w), 1622(w), 1589(m), 1559(w), 1482(s), 1458(sh), 1438(m), 1406(w), 1315(m), 1271(m), 1251(m), 1220(m), 1165(sh), 1151(w), 1129(w), 1091(w), 1033(w), 973(m), 933(w), 903(w), 871(sh), 860(w), 817(m), 756(sh), 742(vs), 733(sh), 726(sh), 699(sh), 661(w), 624(w), 518(w), 496(w), 456(w).

¹H NMR (CDCl₃, ppm): δ = 8.15(d, 1H, 8.7Hz), 8.06(d, 1H, 7.3Hz), 7.74(d, 1H, 8.0Hz), 7.50(dd, 4H, 29.1, 21.6Hz), 7.39 – 7.12(m, 30H), 7.11 – 6.99(m, 2H), 6.89(s, 2H), 6.75(d, 1H, 7.3Hz), 2.30(s, 3H).

¹³C NMR (125 MHz, CDCl₃): δ = 165.8, 165.7, 156.8, 151.9, 143.7, 132.9, 132.0, 129.3, 129.0, 126.9, 125.6, 122.6, 122.5, 120.2, 118.8, 117.5 ppm

³¹P NMR (CDCl₃-d₆): δ = 25.60 ppm.

[Re(*p*-NTol)Br(L²)(PPh₃)₂]ReO₄·PPh₃ (10). (0.52 g of [Re(*p*-NTol)Br₃(PPh₃)₂] and 0.14 g of 2-(2-hydroxyphenyl)benzothiazole yielded 520 mg of **10**; yield 65%). C₇₄H₆₀BrN₂O₅P₃SRe₂ (1634.52): calcd. C 54.38, H 3.70, N 1.71 %; found C 54.61, H 3.79, N 1.65 %.

IR (KBr; ν/cm^{-1}): 3050(w), 1593(w), 1570(sh), 1560(w), 1481(sh), 1469(m), 1443(sh), 1433(m), 1407(w), 1342(w), 1326(w), 1284(w), 1268(w), 1226(w), 1189(w), 1173(w), 1161(w), 1132(w), 1117(w), 1091(m), 1070(w), 1028(w), 1018(w), 997(w), 961(w), 909(vs), 893(s), 848(m), 830(w), 811(w), 766(sh), 743(m), 694(vs), 669(sh), 662(sh), 627(m), 572(w), 559(w), 545(w), 519(s), 493(m), 449(w), 434(w).

¹H NMR (CDCl₃, ppm): δ = 8.06(d, 1H, 8.3Hz), 7.78(d, 1H, 8.5Hz), 7.52(t, 1H, 7.5Hz), 7.39(d, 10H, 12.7Hz), 7.33(t, 8H, 7.3Hz), 7.24(d, 20H, 1.8Hz), 7.17(t, 13H, 7.4Hz), 6.92 – 6.84(m, 2H), 6.74(d, 1H, 8.2Hz) and 2.31(s, 3H).

¹³C NMR (125 MHz, DMSO-d₆): δ = 167.8, 162.0, 157.5, 150.5, 149.9, 137.0, 133.8, 133.6, 131.9, 131.5, 129.5, 129.3, 129.2, 128.9, 126.7 123.9, 123.4, 122.9, 121.7, 121.1, 120.2, 22.07 ppm.

³¹P NMR (CDCl₃-d₆): δ = 25.78, -6.76 ppm.

4.5 Preparation of complexes 11–16

Compound *mer*-[Re(*p*-NTol)X₃(PPh₃)₂] (0.54 mmol) was added to the corresponding phenolate-based ligand (0.60 mmol) in methanol (60 mL) and the reaction mixture was refluxed for 3 h. After that, the solution of NH₄PF₆ (0.19 g, 1.20 mmol) in methanol (5mL) was added and the reaction mixture was refluxed for one hour. The resulting solution was reduced in volume to 10 mL and allowed to cool to room temperature. A brown crystalline precipitate of **11–16** was filtered off and dried in the air. X-ray quality brown crystals were obtained by slow recrystallization from methanol.

[Re(*p*-NTol)Cl(L¹)(PPh₃)₂]PF₆ (11). (0.43 g of [Re(*p*-NTol)Cl₃(PPh₃)₂] and 0.13 g of 2-(2-hydroxy-5-methylphenyl)benzotriazole yielded to 495 mg of **11**; yield 75%). C₅₆H₄₇ClF₆N₄OP₃Re (1220.59): calcd. C 55.11, H 3.88, N 4.59 %; found C 55.37, H 3.94, N 4.46 %. IR (KBr; v/cm⁻¹): 3332(w), 3060(w), 1591(w), 1571(w), 1498(m), m 1481(w), 1434(m), 1350(w), 1334(w), 1299(w), 1265(w), 1252(w), 1210(w), 1188(w), 1176(w), 1160(w), 1140(w), 1118(w), 1091(w), 1071(w), 1028(w), 1017(w), 998(w), 905(w), 858(sh), 837(vs), 785(w), 743(m), 693(s), 651(w), 639(w), 615(w), 557(m), 529(sh), 519(s), 512(sh), 496(w), 482(w), 447(w).

¹H NMR (DMSO-d₆, ppm): δ = 7.91(d, 1H, 8.6Hz), 7.62(t, 3H, 9.1Hz), 7.45-7.28(m, 10H), 7.27-7.14(m, 23H), 6.90(d, 2H, 8.2Hz), 6.68(d, 2H, 8.1Hz), 2.16(s, 3H), 2.09(s, 3H).

¹³C NMR (125 MHz, CDCl₃): δ = 162.0, 158.7, 158.5, 155.0, 153.2, 150.9, 149.9, 143.7, 143.2, 140.5, 134.3, 133.8, 133.6, 133.0, 131.9, 131.6, 130.0, 129.6, 129.4, 128.5, 125.6, 122.7, 122.8, 119.9, 116.7, 115.5, 22.3, 20.5 ppm

³¹P NMR (CDCl₃-d₆): δ = 25.63, -144.20 ppm.

[Re(*p*-NTol)Br(L¹)(PPh₃)₂]PF₆ (12). (0.52 g of [Re(*p*-NTol)Br₃(PPh₃)₂] and 0.13 g of 2-(2-hydroxy-5-methylphenyl)benzotriazole yielded to 480 mg of **12**; yield 70%). C₅₆H₄₇BrF₆N₄OP₃Re (1265.04): calcd. C 53.17, H 3.74, N 4.43 %; found C 53.41, H 3.81, N 4.57 %. IR (KBr; v/cm⁻¹): 3060(w), 1591(w), 1571(w), 1503(sh), 1497(m), 1481(w), 1434(m), 1350(w), 1334(w), 1311(w), 1299(w), 1284(w), 1265(w), 1252(w), 1210(w), 1189(w), 1176(w), 1161(w), 1140(w), 1119(w), 1090(w),

1073(w), 1028(w), 1017(w), 998(w), 985(w), 905(w) 859(sh), 836(vs), 785(w), 742(m), 694(m), 651(w), 638(w), 614(w), 557(m), 529(w), 519(m), 512(sh), 497(w), 446(w).

¹H NMR (DMSO-d₆, ppm): δ = 7.91(d, 1H, 8.6Hz), 7.64(t, 1H, 7.5Hz), 7.36(dd, 8H, 17.2, 10.0Hz), 7.27-7.10(m, 27H), 6.87(d, 2H, 8.2Hz), 6.66(d, 2H, 8.1Hz),

¹³C NMR (125 MHz, DMSO-d₆): δ = 152.9, 151.0, 148.0, 143.8, 142.3, 134.2, 133.7, 133.1, 132.5, 131.6, 131.1, 129.7, 129.1, 128.8, 128.3, 128.0, 127.9, 127.1, 125.9, 122.4, 122.2, 120.3, 116.2, 22.1, 20.5 ppm.

³¹P NMR (DMSO-d₆): δ = 25.61, -144.28 ppm.

[Re(*p*-NTol)Cl(L²)(PPh₃)₂]·PF₆ (13). (0.43 g of [Re(*p*-NTol)Cl₃(PPh₃)₂] and 0.14 g of 2-(2-hydroxyphenyl)benzothiazole yielded to 500 mg of **13**; yield 80%). C₅₆H₄₅ClF₆N₂OP₃ReS (1222.56): calcd. C 55.01, H 3.71, N 2.29 %; found C 55.39, H 3.80, N 2.36 %. IR (KBr; v/cm⁻¹): 3058(w), 1622(w), 1591(w), 1560(w), 1482(sh), 1472(m), 1458(sh), 1435(m), 1406(w), 1340(w), 1316(w), 1289(w), 1272(w), 1251(w), 1214(w), 1188(w), 1178(w), 1156(w), 1129(w), 1095(w), 1030(w), 1014(w), 998(w), 973(w), 878(sh), 839(vs), 745(s), 726(sh), 695(s), 623(w), 556(w), 521(s), 511(sh), 494(sh), 456(w).

¹H NMR (DMSO-d₆, ppm): δ = 8.17(dd, 1H, 12.4, 8.0Hz), 8.07(d, 1H, 8.1Hz), 7.75(d, 1H, 8.7Hz), 7.37-7.12(m, 34H), 6.88(dd, 3H, 16.8, 7.4Hz), 6.75(d, 2H, 8.2Hz), 2.08(s, 3H).

¹³C NMR (125 MHz, DMSO-d₆): δ = 165.8, 165.7, 156.7, 151.8, 134.6, 132.9, 132.0, 131.9, 129.3, 129.2, 128.9, 126.9, 125.6, 122.6, 122.5, 120.2, 118.7, 117.4, 21.2 ppm.

³¹P NMR (DMSO-d₆): δ = 25.78, -144.15 ppm.

[Re(*p*-NTol)Br(L²)(PPh₃)₂]·PF₆ (14). (0.52 g of [Re(*p*-NTol)Br₃(PPh₃)₂] and 0.14 g of 2-(2-hydroxyphenyl)benzothiazole yielded to 500 mg of **14**; yield 80%). C₅₆H₄₅BrF₆N₂OP₃ReS (1267.02): calcd. C 53.08, H 3.58, N 2.21 %; found C 53.34, H 3.63, N 2.43 %. IR (KBr; v/cm⁻¹): 3075(sh), 3056(w), 1591(w), 1572(sh), 1560(sh), 1482(sh), 1471(m), 1458(sh), 1442(m), 1436(m), 1405(w), 1378(w), 1339(m), 1329(sh), 1288w), 1273(w), 1226(w), 1213(w), 1191(w), 1178(w), 1155(w), 1128(w), 1097(w), 1089(w), 1071(w), 1028(w), 1013(w), 998(w), 939(w), 903(w), 878(sh), 838(s), 744(m), 726(sh), 696(m), 661(w), 653(w), 622(w), 573(w), 556(m), 521(m), 511(sh), 493(w), 435(w).

¹H NMR (CDCl₃, ppm): δ = 8.07(d, 1H, 7.9Hz), 7.77(t, 1H, 8.9Hz), 7.52(t, 1H, 7.6Hz), 7.40 – 7.29(m, 8H), 7.29 – 7.13(m, 26H), 6.88(dd, 3H, 11.8, 7.9Hz), 6.74(d, 2H, 8.2Hz) and 2.31(s, 3H).

¹³C NMR (125 MHz, DMSO-d₆): δ = 167.8, 157.6, 149.9, 143.5, 133.8, 131.5, 130.9, 129.8, 129.3, 128.9, 128.5, 128.0, 126.2, 123.5, 123.0, 121.8, 121.2, 118.1, 22.1 ppm.

³¹P NMR (CDCl₃-d₆): δ = 25.71, -144.21 ppm.

[Re(*p*-NTol)Cl(L³)(PPh₃)₂]PF₆·PPh₃ (15). (0.43 g of [Re(*p*-NTol)Cl₃(PPh₃)₂] and 0.13 g of 22-(2-hydroxyphenyl)benzoxazole yielded to 550 mg of **15**; yield 80%). C₇₄H₆₀ClF₆N₂O₂P₄Re (1468.77): calcd. C 60.51, H 4.12, N 1.91%; found C 60.85, H 4.21, N 1.99 %. IR (KBr; v/cm⁻¹): 3053(w), 1605(w), 1594(w), 1570(w), 1560(w), 1530(w), 1481(m), 1460(w), 1434(m), 1369(w), 1337(w), 1314(w), 1272(w), 1257(w), 1245(w), 1187(w), 1173(w), 1161(w), 1139(w), 1117(w), 1092(w), 1071(w), 1029(w), 1018(w), 998(w), 974(w), 940(w), 921(w), 878(sh), 839(vs), 814(sh), 776(w), 764(sh), 753(sh), 744(s), 694(s), 674(sh), 626(w), 589(w), 557(m), 520(m), 511(sh), 494(m), 448(w), 435(w), 416(w). ¹H NMR (CDCl₃, ppm): δ = 7.74(d, 1H, 8.4Hz), 7.56(t, 1H, 7.5Hz), 7.40(d, 9H, 1.3Hz), 7.35(t, 7H, 7.8Hz), 7.31 – 7.14(m, 34H), 6.93(t, 3H, 8.8Hz), 6.76(d, 2H, 8.2Hz) and 2.34(s, 3H). ¹³C NMR (125 MHz, DMSO-d₆): δ = 163.7, 160.8, 156.5, 155.0, 154.9, 153.8, 147.2, 145.8, 144.4, 142.0, 133.7, 132.5, 132.8, 131.9, 129.7, 128.2, 119.9, 118.5, 112.7, 112.3, 22.1 ppm. ³¹P NMR (CDCl₃-d₆): δ = 25.85, -6.82, -144.21 ppm.

[Re(*p*-NTol)Br(L²)(PPh₃)₂]PF₆·PPh₃ (16). (0.52 g of [Re(*p*-NTol)Br₃(PPh₃)₂] and 0.13 g of 2-(2-hydroxyphenyl)benzoxazole yielded to 560 mg of **16**; yield 75%). C₇₄H₆₀BrF₆N₂O₂P₄Re (1513.23): calcd. C 58.73, H 4.00, N 1.85 %; found C 58.94, H 3.89, N 1.78 %. IR (KBr; v/cm⁻¹): 3073(sh), 3053(w), 1605(w), 1594(w), 1570(w), 1560(w), 1530(w), 1481(m), 1460(w), 1434(m), 1369(w), 1342(w), 1313(w), 1272(w), 1257(w), 1245(w), 1188(w), 1173(w), 1139(w), 1092(w), 1072(sh), 1028(w), 1017(w), 998(w), 974(w), 940(w), 921(w), 878(sh), 839(vs), 813(sh), 776(w), 763(sh), 753(sh), 744(s), 694(s), 674(sh), 651(w), 625(w), 589(w), 557(m), 520(m), 511(sh), 494(w), 447(w), 436(w), 419(w). ¹H NMR (CDCl₃, ppm): δ = 7.59(dd, 2H, 17.9, 9.6Hz), 7.40(s, 7H), 7.35(t, 6H, 7.4Hz), 7.22(dt, 33H, 14.7, 9.8Hz), 7.11(s, 3H), 7.05 – 6.87(m, 5H), 6.72(d, 1H, 8.4) and 2.34(s, 3H). ¹³C NMR (125 MHz, DMSO-d₆): δ = 162.9, 160.9, 152.7, 148.3, 142.2, 133.9, 133.5, 132.7, 132.5, 131.9, 129.3, 129.2, 128.9, 120.9, 119.9, 118.3, 112.6, 22.0 ppm. ³¹P NMR (CDCl₃-d₆): δ = 25.74, -6.83, -144.21 ppm.

4.6 Catalytic oxidation of alcohols and alkanes

Catalysts were introduced into the reaction solution in acetonitrile containing a substrate and TBHP. The reactions were typically carried out in air in thermostated Pyrex cylindrical vessels with vigorous stirring; total volume of the reaction solution was 2–5 mL. (**Caution:** the combination of air or molecular oxygen and peroxides with organic compounds at elevated temperatures may be explosive!) Samples of the reaction mixture were taken after certain time intervals, and concentrations of acetophenone were measured using ¹H NMR method (Bruker AMX-400 instrument, 400 MHz). Added to the sample

acetone-*d*₆ was used as a component of the solvent (in addition to acetonitrile); 1,4-dinitrobenzene was a standard. The detection and quantification of the obtained products of the catalytic reactions were made by measuring the areas of peaks corresponding to methyl group from acetophenone (2.6 ppm). Products obtained from octanols and alkanes were analyzed using GC method (chromatograph-3700, fused silica capillary column FFAP/OV-101 20/80 w/w, 30 m × 0.2 mm × 0.3 μm; helium as a carrier gas). The reaction sample was treated with PPh₃ before the analysis.

Conflict of interest

The authors declare no financial interest.

Acknowledgements

The research was co-financed by the National Research and Development Center (NCBiR) under Grant ORGANOMET No: PBS2/A5/40/2014 and the Russian Foundation for Basic Research (grant No. 12-03-00084-a). The authors thank Dr. Yuriy N. Kozlov for helpful discussions.

References

- 1 (a) R. L. Richards, *Coord. Chem. Rev.*, 1996, **154**, 83; (b) M. D. Fryzuk and S. A. Johnson, *Coord. Chem. Rev.*, 2000, **200–202**, 379; (c) K. Mersmann, A. Hauser, N. Lehnert and F. Tuczek, *Inorg. Chem.*, 2006, **45**, 5044; (d) A. J. Keane, P. Y. Zavalij and L. R. Sita, *J. Am. Chem. Soc.* 2013, **135**, 9580.
- 2 (a) J. S. Johnson and R. G. Bergman, *J. Am. Chem. Soc.*, 2001, **123**, 2923; (b) B. F. Straub and R. G. Bergman, *Angew. Chem. Int. Ed.*, 2001, **40**, 4632; (c) Y. Li, Y. Shi and A. L. Odom, *J. Am. Chem. Soc.*, 2004, **126**, 1794; (d) N. Vujkovic, B. D. Ward, A. Maisse-François, H. Wadeohl, P. Mountford and L. H. Gade, *Organometallics*, 2007, **26**, 5522; (e) Z. Zhang, D. Leitch, C. M. Lu, B. O. Patrick and L. L. Schafer, *Chem. Eur. J.*, 2007, **13**, 2012; (f) B. Lian, T. P. Spaniol, P. Horrillo-Martinez, K. C. Hultzsch and J. Okuda, *Eur. J. Inorg. Chem.*, 2009, 429; (g) J. C.-H. Yim and L. L. Schafer, *Eur. J. Org. Chem.*, 2014, 6825.
- 3 (a) S. Abbina, S. Bian, C. Oian and G. Du, *ACS Catal.*, 2013, **3**, 678; (b) G. Du, P. E. Fanwick and M. M. Abu-Omar, *J. Am. Chem. Soc.*, 2007, **129**, 5180; (c) T. V. Truong, E. A. Kastl and G. Du, *Tetrahedron Lett.*, 2011, **52**, 1670.
- 4 M. Mori, *Heterocycles*, 2009, **78**, 281.
- 5 (a) A. P. Duncan and R. G. Bergman, *Chem. Rev.*, 2002, **2**, 431; (b) H. M. Hoyt, F. E. Michael and R. G. Bergman, *J. Am. Chem. Soc.*, 2004, **126**, 1018; (c) R. E. Cowley and P. L. Holland, *Inorg. Chim. Acta*, 2011, **369**, 40; (d) J. R. Webb, S. A. Burgess, T. R. Cundari and T. B. Gunnoe, *Dalton Trans.*, 2013, **42**, 16646.
- 6 (a) T. Gehrmann, G. T. Plundrich, H. Wadeohl and L. H. Gade, *Organometallics*, 2012, **31**, 3346; (b) C. Cheng, D. Chen and Z. Wang, *Chem. Eur. J.* 2013, **19**, 1204; (c) J. Chu, X. Han, C. E. Kefalidis, J. Zhou, L. Maron, X. Leng and Y. Chen, *J. Am. Chem. Soc.*, 2014, **136**, 10894.
- 7 J. Chatt and G. A. Rowe, *J. Chem. Soc.*, 1962, 4019.
- 8 (a) G. R. Clarke, A. J. Nielson and C. E. F. Rickard, *Polyhedron*, 1988, **7**, 117; (b) M. R. Cook, W. A. Herrmann, P. Kiprok and J. Takacs, *J. Chem. Soc., Dalton Trans.*, 1991, 797; (c) I. S. Kolomnikov, Y. D. Koreshkov, T. S. Lobeeva and M. E. Vol'pin, *J. Chem. Soc., Chem. Commun.*, 1979, 1432.
- 9 J. Chatt, J. R. Dilworth, *J. Chem. Soc., Chem. Commun.*, 1972, 519.

- 10 G. K. Lahiri, S. Goswami, L. R. Falvello and A. Chakravorty, *Inorg. Chem.*, 1987, **26**, 3365.
- 11 M. Harman, D. W. A. Sharpe and J. M. Winfield, *Inorg. Nucl. Chem. Lett.*, 1974, **10**, 183.
- 12 E. Deutsch, K. Libson, S. Jurisson and L. F. Lindoy, *Prog. Inorg. Chem.*, 1983, **30**, 75.
- 13 (a) P. C. Bevan, J. Chatt, J. R. Dilworth, R. A. Henderson and G. J. Leigh, *J. Chem. Soc., Dalton Trans.*, 1982, 821; (b) M. W. Bishop, J. Chatt, J. R. Dilworth, B. D. Neaves, P. Dahlstrom, J. Hyde and J. A. Zubieta, *J. Organometal. Chem.* 1981, **213**, 109.
- 14 Y. Takahashi, N. Onoyama, Y. Ishikawa, S. Motojima and K. Sugiyama, *Chem. Lett.*, 1978, 525.
- 15 F. A. Cotton, S. Durow and R. J. Roth, *J. Am. Chem. Soc.*, 1984, **106**, 4749.
- 16 U. Abram and R. Alberto, *J. Braz. Chem. Soc.*, 2006, **17**, 1486.
- 17 (a) M. A. Masood, B. P. Sullivan and D. J. Hogson, *Inorg. Chem.*, 1999, **38**, 5425; (b) M. Bakir, J. A. M. McKenzie and B. P. Sullivan, *Inorg. Chim. Acta*, 1997, **254**, 9; (c) F. Refosco, C. Bolzati, F. Tisato and G. Bandoli, *J. Chem. Soc. Dalton Trans.*, 1998, 923.
- 18 (a) I. Gryca, B. Machura, J. G. Małecki, L. S. Shul'pina, A. J. L. Pombeiro and G. B. Shul'pin, *Dalton Trans.*, 2014, **43**, 5759; (b) B. Machura, I. Gryca, J. G. Małecki, F. Alonso and Y. Moglie, *Dalton Trans.*, 2014, **43**, 2596; (c) B. Machura, M. Wolff and I. Gryca, *Inorg. Chim. Acta*, 2011, **370**, 7; (d) B. Machura, M. Wolff, A. Świtlicka and I. Gryca, *Polyhedron*, 2010, **29**, 2381.
- 19 B. Machura, I. Gryca and M. Wolff, *Polyhedron*, 2012, **31**, 128.
- 20 B. Machura, R. Kruszynski and M. Jaworska, *Polyhedron*, 2006, **25**, 1111.
- 21 B. Machura, M. Wolff and J. Kusz, *Polyhedron*, 2010, **29**, 1619.
- 22 B. Machura and I. Gryca, *Polyhedron*, 2013, **53**, 83.

- 23 (a) V. M. Bereau, S. I. Khan and M. M. Abu-Omar, *Inorg. Chem.*, 2001, **40**, 6767; (b) L. Wei, J. Zubieta and J.W. Babich, *Inorg. Chem.*, 2004, **43** 6445; (c) G. Bandoli, T. I. A. Gerber, J. Perils and J. G. H. du Preez, *Inorg. Chim. Acta*, 1998, **278**, 96; (d) I. Booysen, T. I. A. Gerber, E. Hosten and P. Mayer, *J. Coord. Chem.*, 2007, **60**, 1749; (e) J. B. Arterburn, K. V. Rao, D. M. Goreham, M. V. Valenzuela, M. S. Holguin, K. A. Hall, K. C. Ott and J. C. Bryan, *Organometallics*, 2000, **19**, 1789; (f) G. Bandoli, A. Dolmella, T. I. A. Gerber, J. Perils and J. G. H. du Preez, *Bull. Chem. Soc. Ethiop.*, 2002, **16**, 149; (g) T. I. A. Gerber, D .G. Luzipo and P. Mayer, *J. Coord. Chem.*, 2006, **59**, 1515; (h) J. B. Arterburn, I. M. Fogarty, K. A. Hall, K. C. Ott and J. C. Bryan, *Angew. Chem., Int. Ed.*, 1996, **35**, 2877.
- 24 S. R. Flechter and A.C. Skapski, *J. Chem. Soc., Dalton Trans.*, 1972, 1073.
- 25 F. H. Allen, *Acta Cryst.*, 2002, **B58**, 380.
- 26 (a) J. Muzart, *Tetrahedron*, 2003, **59**, 5789; (b) G. Tojo and M. Fernandez, *Oxidation of Alcohols to Aldehydes and Ketones*; Springer Science, Business Media, Inc.: New York, 2006; c) T. Seki and A. Baiker, *Chem. Rev.*, 2009, **109**, 2409; (d) I. Hermans, E. S. Spier, U. Neuenschwander, N. Turrà and A. Baiker, *Top. Catal.*, 2009, **52**, 1162; (e) M. J. Schultz and M. S. Sigman, *Tetrahedron*, 2006, **62**, 8227; (f) Z. Lounis, A. Riahi, F. Djafri and J. Muzart, *Appl. Catal. A: General*, 2006, **309**, 270; (g) Z. Weng, G. Liao, J. Wang and X. Jian, *Catal. Commun.*, 2007, **8**, 1493; (h) M. D. Tzirakis, I. N. Lykakis, G. D. Panagiotou, K. Bourikas, A. Lycoughiotis, C. Kordulis and M. Orfanopoulos, *J. Catal.*, 2007, **252**, 178; (i) A. Francais, O. Bedel and A. Haudrechy, *Tetrahedron*, 2008, **64**, 2495; (j) F. Shi, M. K. Tse, M.-M. Pohl, J. Radnik, A. Brückner, S. Zhang and M. Beller, *J. Mol. Catal., A: Chem.*, 2008, **292**, 28; (k) A. M. Khenkin and R. Neumann, *J. Am. Chem. Soc.*, 2008, **130**, 14474; (l) P. J. Figiel, A. M. Kirillov, Y. Y. Karabach, M. N. Kopylovich and A. J. L. Pombeiro, *J. Mol. Catal., A: Chem.*, 2009, **305**, 178; (m) T. Hida and H. Nogusa, *Tetrahedron*, 2009, **65**, 270; (n) K. T. Mahmudov, M. N. Kopylovich, M. F. C. G. da Silva, P. J. Figiel, Y.Y. Karabach and A. J. L. Pombeiro, *J. Mol. Catal., A: Chem.*, 2010, **318**, 44; (o) M. N. Kopylovich, K. T. Mahmudov, M. F. C. G. da Silva, P. J. Figiel, Y. Y. Karabach, M. L. Kuznetsov, K. V. Luzyanin and A. J. L. Pombeiro, *Inorg. Chem.* 2011, **50**, 918; (p) R. Cang, B. Lu, X. Li, R. Niu, J. Zhao and Q. Cai, *Chem. Eng. Sci.*, 2015, **137**, 268; (q) W. Dai, Y. Lv, L. Wang, S. Shang, B. Chen, G. Li and S. Gao, *Chem. Commun.*, 2015, **51**, 11268; (r) T. Chen and C. Cai, *Synth. Commun.*, 2015, **45**, 1334; (s) S. Dinda, A. Genest and N. Rösch, *ACS Cat.*, 2015, **5**, 4869.

27 Recent reviews on alkane activation and oxygenation: (a) J. Muzart, *Mini-Rev. Org. Chem.*, 2009, **6**, 9; (b) V. N. Cavaliere, D. J. Mindiola, *Chem. Sci.*, 2012, **3**, 3356; (c) A. Sivaramakrishna, P. Suman, E. V. Goud, S. Janardan, C. Sravani, T. Sandep, K. Vijayakrishna and H. S. Clayton, *J. Coord. Chem.*, 2013, **66**, 2091; (d) A. B. Sorokin, *Chem. Rev.*, 2013, **113**, 8152; (e) L. M. D. R. S. Martins and A. J. L. Pombeiro, *Coord. Chem. Rev.*, 2014, **265**, 74; (f) N. J. Gunsalus, M. M. Konnivk, B. G. Hashiguchi and R. A. Periana, *Isr. J. Chem.*, 2014, **54**, 1467; (g) D. Munz and T. Strassner, *Inorg. Chem.*, 2015, **54**, 5043; (h) E. S. Rudakov and G. B. Shul'pin, *J. Organometal. Chem.*, 2015, **793**, 4; (i) A. F. Shestakov and N. F. Goldshleger, *J. Organometal. Chem.*, 2015, **793**, 17; (j) A. A. Shteinman, *J. Organometal. Chem.*, 2015, **793**, 34; (k) R. H. Crabtree, *J. Organometal. Chem.*, 2015, **793**, 41; (l) J. A. Labinger and J. E. Bercaw, *J. Organometal. Chem.*, 2015, **793**, 47; (m) E. G. Chepaikin and V. N. Borshch, *J. Organometal. Chem.*, 2015, **793**, 78; (n) E. P. Talsi, R. V. Ottenbacher and K. P. Bryliakov, *J. Organometal. Chem.*, 2015, **793**, 102.

28 Selected recent original papers on metal-catalyzed hydrocarbon oxidations with peroxides including catalysis by rhenium complexes: (a) U. Schuchardt, D. Mandelli and G. B. Shul'pin, *Tetrahedron Lett.*, 1996, **37**, 6487; (b) G. Bianchini, M. Crucianelli, F. De Angelis, V. Neri and R. Saladino, *Tetrahedron Lett.*, 2004, **45**, 2351; (c) J. H. Espenson, *Coord. Chem. Rev.*, 2005, **249**, 329; (d) G. Bianchini, M. Crucianelli, C. Canevali, C. Crestini, F. Morazzoni and R. Saladino, *Tetrahedron*, 2006, **62**, 12326; (e) G. Bianchini, M. Crucianelli, C. Crestini and R. Saladino, *Topics Catal.*, 2006, **40**, 221; (f) C. Freund, W. Herrmann and F. E. Kühn, *Topics Organometal. Chem.*, 2007, **22**, 39; (g) K. R. Jain and F. E. Kühn, *J. Organometal. Chem.*, 2007, **692**, 5532; (h) J. M. Gonzales, R. Distasio, Jr., R. A. Periana, W. A. Goddard III and J. Oxgaard, *J. Am. Chem. Soc.*, 2007, **129**, 15794; (i) G. B. Shul'pin, D. V. Muratov, L. S. Shul'pina, A. R. Kudinov, T. V. Strelkova and P. V. Petrovskiy, *Appl. Organometal. Chem.*, 2008, **22**, 684; (j) T. F. S. Silva, E. C. B. A. Alegria, L. M. D. R. S. Martins and A. J. L. Pombeiro, *Adv. Synth. Catal.*, 2008, **350**, 706; (k) R. Saladino, V. Nery, A. Farina, C. Crestini, L. Nencioni and A. T. Palamara, *Adv. Synth. Catal.*, 2008, **350**, 321; (l) A. B. Sorokin, E. V. Kudrik and D. Bouchu, *Chem. Commun.*, 2008, 2562; (m) R. R. Fernandes, M. V. Kirillova, J. A. L. da Silva, J. J. R. Frausto da Silva, A. J. L. Pombeiro, *Appl. Catal., A: General*, 2009, **353**, 107; (n) M. L. Kuznetsov and A. J. L. Pombeiro, *Inorg. Chem.*, 2009, **48**, 307; (o) B. Monteiro, S. Gago, S. S. Balula, A. A. Valente, I. S. Goncalves and M. Pillinger, *J. Mol. Catal., A: Chem.*, 2009, **312**, 23; (p) C. Detoni, N. M. F. Carvalho, D. A. G. Aranda, B. Louis, O. A. C. Antunes, *App. Catal., A: General*, 2009, **365**, 281; (q) E. V. Kudrik, P. Afanasiev, L. X. Alvarez, P. Dubourdeaux, M. Clémancey, J.-M. Latour, G. Blondin, D. Bouchu, F. Albrieux, S. E. Nefedov and A. B. Sorokin, *Nature Chem.*, 2012, **4**, 1024; (r) A. P. C. Ribeiro, L. M. D. R. S. Martins, S. Hazra and A. J. L. Pombeiro, *C. R. Chimie*, 2015, **18**, 758; (s) L. X. Alvarez and A. B. Sorokin, *J.*

Organometal. Chem., 2015, **793**, 139; (t) L. S. Shul'pina, A. R. Kudinov, D. Mandelli, W. A. Carvalho, Y. N. Kozlov, M. M. Vinogradov, N. S. Ikonnikov and G. B. Shul'pin, *J. Organometal. Chem.*, 2015, **793**, 217; (u) S. M. Paradine, J. R. Griffin, J. Zhao, A. L. Petronico, S. M. Miller and M. C. White, *Nature Chem.*, 2015, DOI: 10.1038/NCHEM.2366

29 (a) Y. N. Kozlov, G. V. Nizova and G. B. Shul'pin, *J. Mol. Catal., A: Chem.*, 2005, **227**, 247; (b) G. B. Shul'pin and Y. N. Kozlov, *Org. Biomol. Chem.*, 2003, **1**, 2303; (c) G. B. Shul'pin, J. Gradinaru and Y. N. Kozlov, *Org. Biomol. Chem.*, 2003, **1**, 3611.

30 Reviews: (a) A. E. Shilov and G. B. Shul'pin, *Chem. Rev.*, 1997, **97**, 2879; (b) *Biomimetic Oxidations Catalyzed by Transition Metal Complexes*; B. Meunier (Ed.); Imperial College: London, 2000; (c) A. E. Shilov, G. B. Shul'pin, *Activation and Catalytic Reactions of Saturated Hydrocarbons in the Presence of Metal Complexes*; Kluwer Academic Publishers: Dordrecht/Boston/London, 2000; (d) G. B. Shul'pin, "Oxidations of C–H Compounds Catalyzed by Metal Complexes", in *Transition Metals for Organic Synthesis*; M. Beller and C. Bolm (Eds.), 2nd edition, Wiley–VCH: Weinheim/New York, Vol. 2, Chapter 2.2, 2004, pp 215–242.

31 Original papers: (a) I. V. Spirina, V. N. Alyasov, V. N. Glushakova, N. A. Skorodumova, V. P. Sergeeva, N. V. Balakshina, V. P. Maslennikov, Y. A. Aleksandrov and G. A. Razuvaev, *Zhurn. Org. Khim.*, 1982, **18**, 1796 (in Russian); (b) M. Bressan, A. Morville and G. Romanello, *J. Mol. Catal.*, 1992, **77**, 283; (c) T. Kojima, H. Matsuo and Y. Matsuda, *Inorg. Chim. Acta*, 2000, **300–302**, 661; (d) D. Chatterjee, A. Mitra and S. Mukherjee, *J. Mol. Catal., A: Chem.*, 2001, **165**, 295; (e) R. L. Brutchev, I. J. Drake, A. T. Bell and T. D. Tilley, *Chem. Commun.*, 2005, 3736; (f) P. Karandikar, A. J. Chandwadkar, M. Agashe, N. S. Ramgir and S. Sivasanker, *Appl. Catal., A: General*, 2006, **297**, 220.

32 (a) G. B. Shul'pin, *J. Mol. Catal. A: Chem.*, 2002, **189**, 39; (b) G. B. Shul'pin, *C. R. Chim.*, 2003, **6**, 163; (c) G. B. Shul'pin, *Mini-Rev. Org. Chem.*, 2009, **6**, 95; (d) G. B. Shul'pin, Y. N. Kozlov, L. S. Shul'pina, A. R. Kudinov and D. Mandelli, *Inorg. Chem.*, 2009, **48**, 10480; (e) G. B. Shul'pin, *Org. Biomol. Chem.*, 2010, **8**, 4217; (f) G. B. Shul'pin, Y. N. Kozlov, L. S. Shul'pina and P. V. Petrovskiy, *Appl. Organometal. Chem.*, 2010, **24**, 464; (g) G. B. Shul'pin, *Dalton Trans.*, 2013, **42**, 12794.

33 (a) G. B. Shul'pin, Y. N. Kozlov, G. V. Nizova, G. Süss-Fink, S. Stanislas, A. Kitaygorodskiy and V. S. Kulikova, *J. Chem. Soc. Perkin Trans. 2*, 2001, 1351; (b) Y. N. Kozlov, V. B. Romakh, A.

Kitaygorodskiy, P. Buglyó, G. Süss-Fink and G. B. Shul'pin, *J. Phys. Chem. A*, 2007, **111**, 7736; (c) M. V. Kirillova, M. L. Kuznetsov, V. B. Romakh, L. S. Shul'pina, J. J. R. Fraústo da Silva, A. J. L. Pombeiro and G. B. Shul'pin, *J. Catal.*, 2009, **267**, 140; (d) M. M. Vinogradov, Y. N. Kozlov, D. S. Nesterov, L. S. Shul'pina, A. J. L. Pombeiro, G. B. Shul'pin, *Catal. Sci. Technol.*, 2014, **4**, 3214; (e) M. M. Vinogradov, L. S. Shul'pina, Y. N. Kozlov, A. R. Kudinov, N. S. Ikonnikov and G. B. Shul'pin, *J. Organometal. Chem.*, 2015, **784**, 52-61; (f) G. B. Shul'pin, Y. N. Kozlov, L. S. Shul'pina, W. Carvalho and D. Mandelli, *RSC Adv.*, 2013, **3**, 15065; (g) G. B. Shul'pin, A. R. Kudinov, L. S. Shul'pina and E. A. Petrovskaya, *J. Organometal. Chem.*, 2006, **691**, 837; (h) G. B. Shul'pin, M. V. Kirillova, Y. N. Kozlov, L. S. Shul'pina, A. R. Kudinov and A. J. L. Pombeiro, *J. Catal.*, 2011, **277**, 164; (i) G. B. Shul'pin, G. V. Nizova, Y. N. Kozlov, L. Gonzalez Cuervo and G. Süss-Fink, *Adv. Synth. Catal.*, 2004, **346**, 317; (j) G. V. Nizova, B. Krebs, G. Süss-Fink, S. Schindler, L. Westerheide, L. Gonzalez Cuervo and G. B. Shul'pin, *Tetrahedron*, 2002, **58**, 9231; (k) E. E. Karslyan, L. S. Shul'pina, Y. N. Kozlov, A. J. L. Pombeiro and G. B. Shul'pin, *Catal. Today*, 2013, **218–219**, 93; (l) V. B. Romakh, B. Therrien, G. Süss-Fink and G. B. Shul'pin, *Inorg. Chem.*, 2007, **46**, 3166; (m) D. Mandelli, K. C. Chiacchio, Y. N. Kozlov, G. B. Shul'pin, *Tetrahedron Lett.*, 2008, **49**, 6693; (n) M. L. Kuznetsov, B. G. M. Rocha, A. J. L. Pombeiro and G. B. Shul'pin, *ACS Catal.*, 2015, **5**, 3823. (o) A. M. Kirillov, M. V. Kirillova, L. S. Shul'pina, P. J. Figiel, K. R. Gruenwald, M. F. C. G. da Silva, M. Haukka, A. J. L. Pombeiro and G. B. Shul'pin, *J. Mol. Catal. A: Chem.*, 2011, **350**, 26; (p) M. M. Vinogradov, Y. N. Kozlov, A. N. Bilyachenko, D. S. Nesterov, L. S. Shul'pina, Y. V. Zubavichus, A. J. L. Pombeiro, M. M. Levitsky, A. I. Yalymov, G. B. Shul'pin, *New J. Chem.*, 2015, **39**, 187; (q) M. V. Kirillova, A. M. Kirillov, D. Mandelli, W. A. Carvalho, A. J. L. Pombeiro and G. B. Shul'pin, *J. Catal.*, 2010, **272**, 9.

34 J. Chatt, J. D. Garforth and N. P. Johnson, G. A. Rowe, *J. Chem. Soc.*, 1964, 1012.

35 CrysAlis RED, Oxford Diffraction Ltd, Version 1.171.33.46, 2003.

36 (a) G. M. Sheldrick, *SHELXS-97. Program for Crystal Structure Resolution*. Univ. of Göttingen: Göttingen, Germany, 1997; (b) G. M. Sheldrick, *SHELXL-97. Program for Crystal Structures Analysis*. Univ. of Göttingen: Göttingen, Germany, 1997.

Graph. Abstr.:

Text:

The reactions of *mer*-[Re(*p*-NTol)X₃(PPh₃)₂] (X= Cl, Br) with chelating phenolate-based ligands gave 16 various new *p*-tolylimido rhenium(V) complexes. Interestingly, only a few of them exhibited high catalytic activity in oxidation of alcohols with *tert*-butyl hydroperoxide (TBHP).

